

LifeSentence: Language models can encode human life course trajectories from longitudinal panel data.

Samuel Liu, Muchen Xi, William Yeoh, Joshua J. Jackson

May 5, 2026

Abstract

Forecasting human life outcomes is important to gain insights into how individuals attain long and healthy lives. Conventional statistical approaches yield limited accuracy, potentially due to discarding the sequential structure of the life course. Modern methods such as transformer architectures require large scale training data that most longitudinal panel studies lack. Here we introduce LifeSentence, a model for life-course reasoning that bridges large language models with longitudinal panel data. By representing each life event as a structured natural-language record and instruction-tuning a pretrained 24-billion-parameter language model across an 18-task evaluation taxonomy spanning prediction, robustness and reasoning, LifeSentence supplements panel data with distributional knowledge already encoded during pretraining. Trained on approximately 65,000 individuals from the German Socio-Economic Panel—roughly 45 times fewer than prior transformer-based approaches—LifeSentence outperforms classical and deep learning baselines across all task families, achieving a threefold improvement in joint event-and-timing prediction from best baselines and 91.2% Kendall’s tau when reconstructing chronological order from timestamp-stripped event sets. Without explicit supervision, the model recovers documented patterns of social stratification, including the education premium, the gender wage gap and the motherhood penalty, from discrete event sequences alone. A natural-language interface further enables qualitatively new research queries, such as connecting an early-life history to a specified late-life endpoint, establishing LifeSentence as both a predictive tool and a probe for counterfactual exploration of human biographies.

Introduction

Accurately forecasting the trajectory of a human life provides foundational insights necessary to understand how individuals can achieve long, healthy, and happy lives.^{1–3} Yet despite decades of inquiry, the predictive accuracy of standard models remains modest,^{4–6} suggesting that prevailing analytical paradigms do not capture the high-dimensional, sequential logic of human existence. The necessity of studying life trajectories spans multiple disciplines.^{7,8} Shocks accumulate across the entire lifespan, with critical periods linking early-life conditions to late-life endpoints.^{9,10} Cumulative advantage specifies how small initial differences compound over time,¹¹ while social clocks describe normative event timing as a mechanism of social control.¹² Collectively, these frameworks establish that a life is a dynamic sequence shaped by timing, context, and accumulated experiences.^{13,14}

Traditional statistical tools discard sequential information, flattening the rich temporal structure of the life course.^{15,16} The Fragile Families Challenge revealed that even sophisticated machine learning struggled to predict life outcomes.⁴ Transformer architectures^{17,18} offered a possible solution.^{19–21} The life2vec study²² validated this approach by training a BERT-like transformer on registry data covering six million Danish citizens, demonstrating that temporal event sequences carry predictive signal about mortality and other life outcomes. However, life2vec exposed a fundamental constraint: training transformers from scratch requires large datasets.^{23,24} Major longitudinal panel studies track across a wider range of variables, but only across tens of thousands rather than millions of participants.

Here, we introduce LifeSentence, a foundation model for life-course reasoning that bridges large language models with longitudinal panel data. Instead of learning from scratch, LifeSentence represents each event as a structured natural-language description and instruction-tunes a pretrained large language model on life-course prediction tasks. Because the pretrained language model already encodes distributional knowledge about the semantic relationships among concepts such as education levels, occupations, and health conditions, fine-tuning only needs to teach the model how they relate to one another across a biography.^{25–27}

LifeSentence outperforms traditional models across an 18-task evaluation taxonomy²⁸ using approximately 65,000 individuals, about 15 times fewer than life2vec. Beyond predictive accuracy, LifeSentence reveals that the sequential structure of human lives encodes far more information about social stratification than previous analyses have extracted.^{4,29} Without any explicit supervision linking specific demographics to outcomes, the model’s generated trajectories reproduce well-documented patterns of socioeconomic stratification, including the education income premium previously established in the literature,^{30,31} the gender wage gap,^{32,33} and the motherhood penalty from event sequences alone,^{34,35} indicating that the co-occurrence structure of discrete life events is sufficient to recover known patterns of socioeconomic stratification. These representations, combined with a natural-language interface that enables qualitatively new research queries ("generate all events until retirement," "connect this early history to this late-life state"), establish LifeSentence as both a predictive tool and a probe for what-if exploration of life-course sequences.

Results

Model Approach

We represent individual lives as temporally ordered sequences of discrete life events—what we term LifeSentences—drawn from the German Socio-Economic Panel (SOEP),^{36,37} a longitudinal household survey spanning decades of observation (Fig. 1a). A LifeSentence encodes a biography: a woman completes secondary school at 18, begins an apprenticeship, enters full-time employment as a nurse, marries at 26, has two children, is diagnosed with hypertension at 52, and retires at 63: each event recorded with its associated details, the individual's age, and calendar year. Events span education (school transitions, certificates, degrees), employment (occupational changes, position levels, retirement), family (marriages, divorces, childbirths, widowhood), and health (diagnosed conditions, death). Alongside discrete events, periodic measurements of continuous state variables (income, life satisfaction, health satisfaction, and occupational prestige) provide a complementary portrait of an individual's circumstances over time.

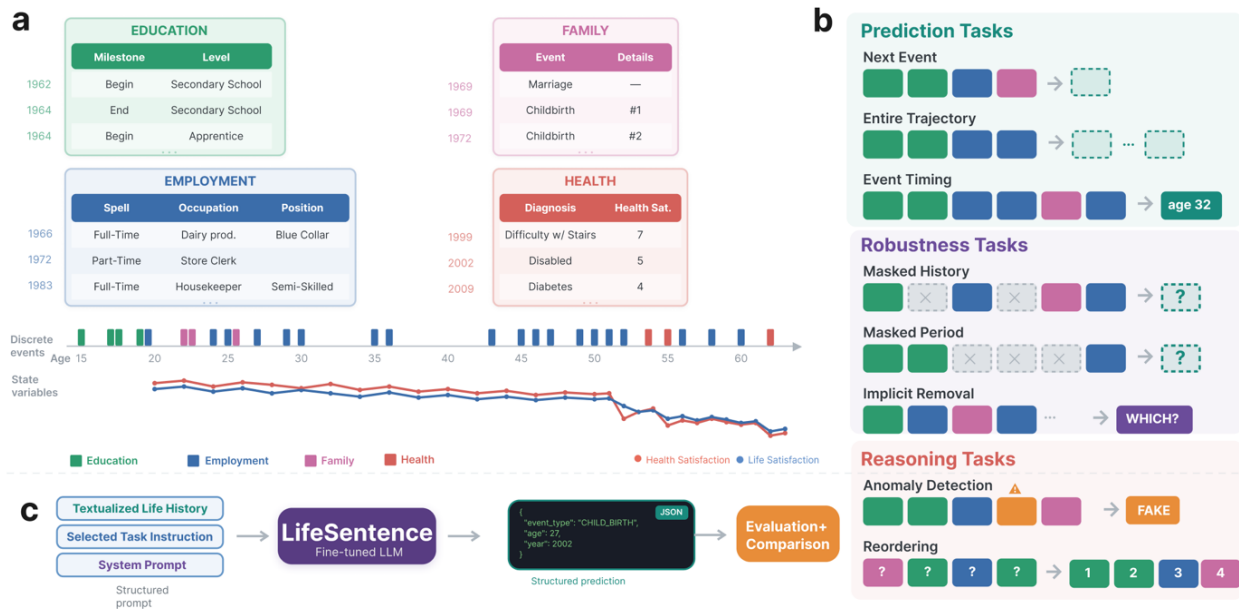


Figure 1 — Overview of the LifeSentence framework. (a) A life sentence encodes an individual's complete biography as a temporally ordered sequence of discrete life events spanning education, employment, family, and health domains. Each event is recorded with its associated details, the individual's age, and the calendar year. Alongside discrete events are periodic measurements of continuous state. (b) The 18-task evaluation taxonomy, organized into three families. Prediction tasks assess forecasting capacity over varying horizons. Robustness tasks test resilience to incomplete information through masked events, redacted time periods, and silent deletions. Reasoning tasks probe structural understanding of biography itself, including anomaly detection and reordering. (c) The inference pipeline. A structured life history, task-specific instruction, and system prompt are concatenated into a single natural-language input. The fine-tuned model generates a structured JSON prediction, which is evaluated against ground-truth trajectories.

Each life event is represented not as a categorical index but as a structured natural-language record, using occupation names, education levels, and diagnostic terms that carry semantic content. This representation allows the model to exploit distributional knowledge already present in a pretrained large language model^{38,39}: the relationship between "apprenticeship" and "vocational certificate" need not be learned from panel data alone. We fine-tune Mistral Small 3.1 (24B parameters) using Low-Rank Adaptation⁴⁰ on the 18 life-course prediction tasks described below. A structured life history, task instruction, and system prompt are concatenated into a single input; the model generates a structured JSON prediction evaluated against ground-truth trajectories (Fig. 1c).

LifeSentence is evaluated across an 18-task taxonomy organized into three families of increasing inferential demand (Fig. 1b). Prediction tasks^{4,22} assess forecasting capacity: predicting next events, generating full trajectories, forecasting to a given year, estimating transition timing. Robustness tasks test resilience to incomplete information by masking events, redacting time periods, or silently removing observations: conditions mirroring gaps common in panel data.^{41,42} Reasoning tasks probe structural understanding: detecting anomalous events, imputing silently removed events, recovering chronological order from shuffled sequences without timestamps, and translating discrete event sequences into the continuous socioeconomic trajectories they produce.

Model	Event Accuracy	Joint Accuracy	Conditional Mean Absolute Error (Years)
LifeSentence	61.6% [61.4-61.8%]	35.3% [35.1-35.5%]	1.15 [1.14-1.17]
XGBoost	58.2% [58.0-58.5%]	15.0% [14.8-15.1%]	1.78 [1.77-1.79]
LSTM	56.4% [56.1-56.6%]	11.6% [11.5-11.8%]	2.30 [2.29-2.31]
GRU	56.5% [56.3-56.7%]	13.8% [13.6-13.9%]	2.23 [2.21-2.24]
Logistic	52.9% [52.7-53.1%]	8.6% [8.4-8.7%]	2.22 [2.21-2.23]
Transformer	50.4% [50.1-50.6%]	8.8% [8.6-8.9%]	2.81 [2.80-2.83]

Table 1. Predictive performance on the next-event task. Comparison of LifeSentence against traditional (Logistic Regression, XGBoost) and deep learning (LSTM, GRU, Transformer) baselines. Metrics reported include Event Accuracy (correct prediction of event type), Joint Accuracy (correct prediction of both event type and age), and Conditional Mean Absolute Error (MAE, temporal error in years given a correct event prediction). 95% confidence intervals (calculated via 1,000 bootstrap samples) are provided in brackets.

LifeSentence predicts life events with high fidelity

We first assessed LifeSentence by evaluating next-event prediction: given an individual's observed history truncated at a random point, predict both the type and timing of the immediately following event.

LifeSentence outperforms all baselines across every metric (Table 1). The model achieves a joint accuracy of 35.3% (correctly predicting both the specific event type and the age at which it occurs), representing a threefold improvement over the closest deep learning baseline and more than double the next-best model. When the event type is predicted correctly, LifeSentence places it within 1.15 years of the true age, compared with 1.78 years or worse for all other baselines.

Performance varies systematically across the life course (Supplementary Fig. 1a–c). All models experience reduced accuracy during the 20–30 age range, consistent with characterizations of emerging adulthood as a dense period of life events.^{43–45} LifeSentence maintains higher accuracy throughout this period, with joint accuracy remaining above approximately 25% even at peak volatility, whereas baselines fall below 10%. Performance is consistent across birth cohorts from the 1930s through the 2000s (Supplementary Fig. 2d–f), indicating that the model captures generalizable temporal dependencies rather than cohort-specific artifacts. Analysis by event type reveals that LifeSentence performs well on both socially normative structured events (education completion) and more variable transitions (job changes) (Supplementary Fig. 2a–c). Of particular note is mortality prediction: LifeSentence predicts death as the next event with 29.8% accuracy, nearly threefold higher than the next-best baseline (XGBoost at 10.3%). When the model fails to predict death, it nearly always predicts a medical diagnosis instead, which is contextually coherent given that illness frequently precedes death in the observed data. This error pattern is consistent with the model having learned the temporal dependency structure between event types—specifically, the illness–death sequence—rather than relying on marginal event frequencies alone. Analysis of immediate next-event transition probabilities confirms this: LifeSentence's transition probability error is threefold lower than all baselines (Supplementary Fig. 3a–c). Baselines fail to learn, for example, that military service start is almost always followed by service end. These one-step transition results establish that the model has appropriately captured shot-range event-transition dependencies.

Trajectory generation maintains structural accuracy over long horizons

Next-event prediction assesses one step ahead local accuracy. To determine whether LifeSentence maintains coherent narrative arcs over longer horizons, we evaluated its capacity for complete trajectory generation: predicting the full sequence of remaining life events from a truncation point through the end of an individual's observed history. The combinatorial space of trajectories is large. ⁴⁷ With 20 event types across a typical 40-year horizon, the space of possible trajectories is large; 96% of trajectories in our test set are unique by the eighth event (Supplementary Fig. 5), meaning the model cannot rely on memorized templates. On average, each test case requires predicting the next 23 years of an individual's life.

Two illustrative cases are presented in Figure 2, one with a smaller input history (truncated at age 18) and one with a more extensive input history (truncated at age 29). For both, LifeSentence generates a trajectory that closely mirrors the ground truth. Baseline models reveal characteristic failures: the transformer degenerates into a dense repetitive loop of events, while XGBoost recovers some of the correct event types but at inappropriate time intervals.

Quantitative evaluation confirms this advantage across multiple dimensions of trajectory accuracy (Supplementary Table 2). LifeSentence achieves a Jaccard similarity ⁴⁸ of 0.627 for event-type overlap and a Levenshtein distance ⁴⁹ of 8.10—meaning generated trajectories require roughly eight edits to match reality, compared with 20 or more for deep learning baselines. Full metric comparisons, including temporal displacement (Wasserstein distance) ⁵⁰ and event-frequency fidelity (Multiset Jaccard) ⁵¹, are reported in Supplementary Table 2.

LifeSentence also reproduces the non-uniform temporal distribution of life events, accurately capturing elevated event density between ages 25 and 30 (Supplementary Fig. 6), while baseline models either do not capture the appropriate peak or overestimate event frequency. Kernel density estimates of age at childbirth, marriage, and death closely track the empirical distributions, while baselines exhibit systematic temporal misalignment (Fig. 3). Beyond aggregate distributional fidelity, the model internalizes complex conditional probabilities: female trajectories exhibit elevated probability of transitioning to part-time employment following the birth of a child compared to men, mirroring the ground-truth pattern ^{34,52} without explicit supervision of this interaction (Supplementary Fig. 7). Direct analysis of generative diversity confirms that LifeSentence produces a substantially wider array of distinct biographical sequences and lower rates of repetitive looping compared to baseline models (Supplementary Fig. 8). Taken together, these results demonstrate that LifeSentence generates diverse trajectories rather than collapsing to a modal sequence.

Applied life-course research rarely calls for unconstrained event generation. Rather, research questions are typically centered around specific events (e.g., diagnosis) ⁵³ or knowing what happened between two observations years apart. These questions impose temporal boundaries, type-specific targets, or structural endpoints that require trajectories satisfying explicit constraints while maintaining narrative coherence. Critically, constraints requiring semantic comprehension ("predict until the next diagnosis," "connect this early history to this late-life state") are difficult to express without a natural-language interface.

We evaluated LifeSentence on six constrained generation tasks spanning three constraint families: count and type-targeted generation (predict the next three events, predict until a specific event, predict when a specific event will happen), temporal-boundary generation (predict until a specific

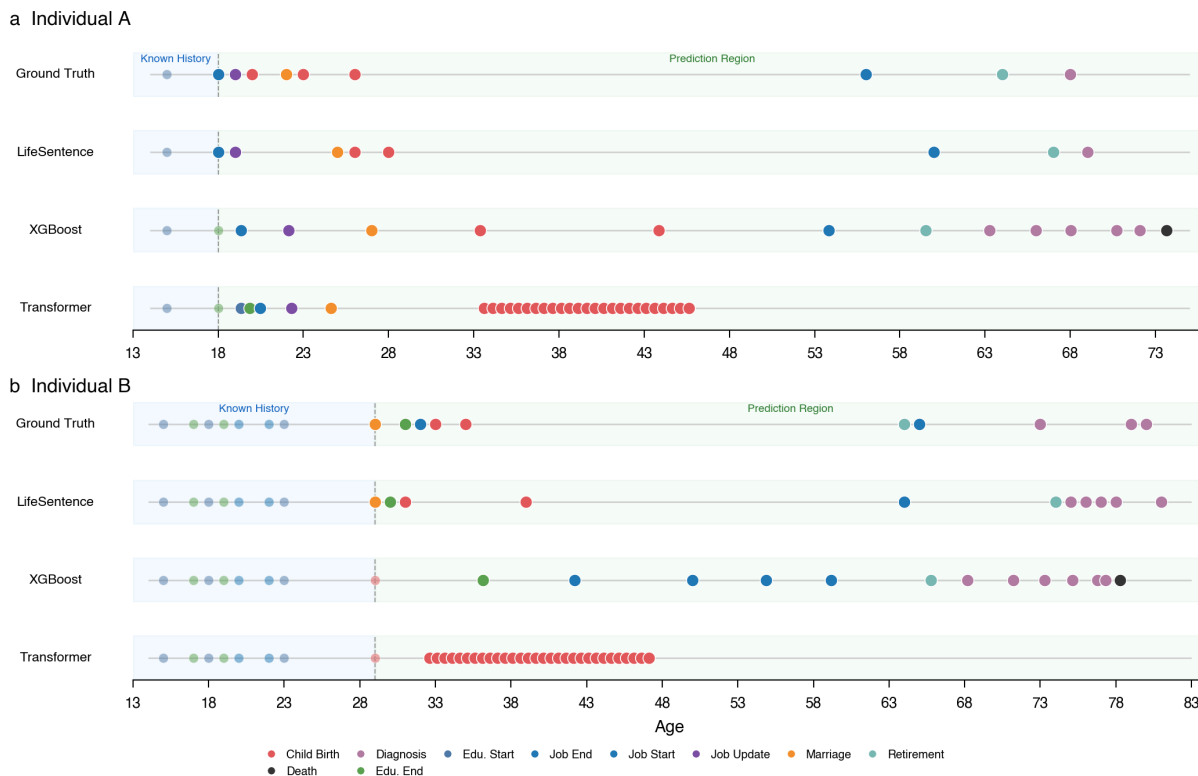


Figure 2 — Trajectory generation across models for two individuals. Comparison of predicted life trajectories from LifeSentence, XGBoost, and a from-scratch Transformer against ground truth. Events prior to the truncation point (dashed line) constitute the observed history (blue shading); events to the right are model predictions (green shading) or ground-truth future events (top row of each panel). (a) Individual A, truncated at age 18 with a prediction horizon spanning approximately 55 years. LifeSentence produces a trajectory that closely mirrors the ground truth in both event composition and temporal spacing, capturing education completion, marriage, childbirths, a long period of occupational stability, retirement, and a late-life diagnosis. XGBoost recovers several correct event types but distributes them unevenly. The from-scratch Transformer exhibits mode collapse, degenerating into a dense repetitive loop of events. (b) Individual B, truncated at age 29. LifeSentence again recovers the major biographical arc with plausible temporal spacing. The Transformer again collapses into repetitive early-life generation, while XGBoost misses key events like marriage.

year, predict what will happen in a certain year), and endpoint-conditioned interpolation (generate trajectory between one partial trajectory and a future state). Full metrics for all six tasks are reported in Supplementary Tables 3a–b. On generation to a specified milestone task, LifeSentence satisfies the termination constraint in 99.3% of cases and achieves a Jaccard of 0.650, compared with the best baseline (LSTM) at 79.2% constraint satisfaction and 0.543 Jaccard (Supplementary Table 3b). Baselines struggle because they lack any mechanism for conditioning generation on a semantic target; they just generate until the target appears. LifeSentence maintains a similar advantage on temporal-boundary generation, achieving a Jaccard of 0.559 on the predict-up-to-year task versus 0.441 for the best baseline.

The remaining three tasks require semantic comprehension of natural-language instructions and are evaluable only for LifeSentence. When asked to predict the timing of a specific future event type, LifeSentence achieves a mean error of 4.23 years. When asked to generate only events occurring during a specific future calendar year, it achieves a Jaccard of 0.429. In the most structurally

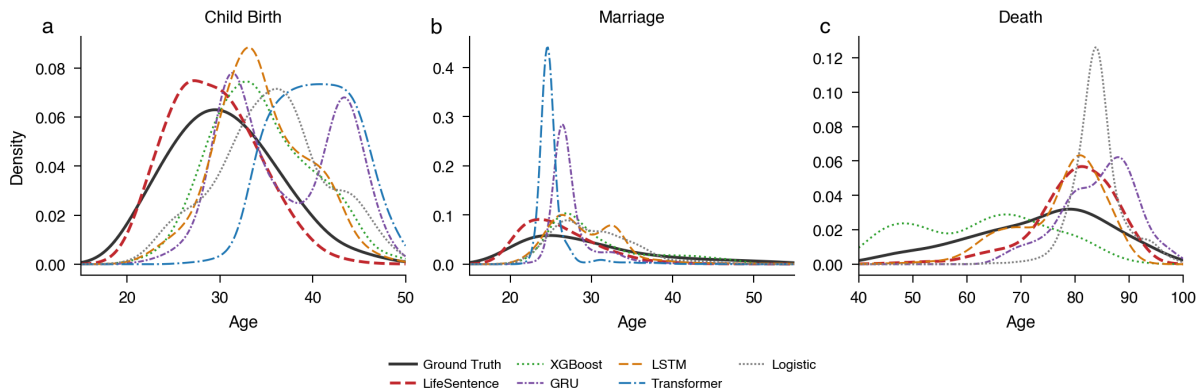


Figure 3— **Macro-structural fidelity of generated life events.** Kernel density estimation plots comparing the age-at-event distributions for (a) Childbirth, (b) Marriage, and (c) Death across Ground Truth, LifeSentence, and baseline models. LifeSentence closely approximates the modal peaks and temporal width of the empirical distributions, whereas other baselines exhibit temporal misalignment.

demanding task (endpoint-conditioned interpolation), the model receives an individual's history up to age 25 and a single anchor event around age 65, then generates the intervening four decades. LifeSentence recovers this missing mid-life trajectory with a Jaccard of 0.587. An illustrative example (Supplementary Fig. 9) shows the model receiving an individual's history through age 25 and a single endpoint (a diagnosis at age 66) and generating the intervening four decades. The model can generate a mid-life sequence of career entry, marriage, childbirths, and eventual retirement that is consistent with both the early history and the late-life endpoint.

LifeSentence internalizes the temporal logic of the life course

The preceding sections evaluated LifeSentence on forward-looking tasks: predicting future events, generating trajectories, and satisfying temporal or semantic constraints during generation. These results establish that the model produces accurate forecasts, but they leave open a distinct question: has the model acquired genuine structural understanding of biographical logic, or is it exploiting surface-level statistical regularities to generate plausible-looking outputs.^{54,55} To probe this, we designed tasks that require no prediction of the future at all, only comprehension of the past.

In the anomaly detection task, we insert a single foreign event randomly drawn from the full event pool into an individual's trajectory, then ask the model to identify it. LifeSentence identifies the anomaly with 93.9% accuracy, demonstrating that it has learned not just what events occur in human lives, but which events belong together within a single life. Events embedded within tight institutional sequences like military service and educational transitions are detected at near-perfect rates because these events generate rigid contextual expectations.⁴⁷ Relationship events such as divorce and marriage prove hardest to detect, because their timing and occurrence vary more substantially⁵⁶ across individuals, so a foreign instance can plausibly pass as authentic (Supplementary Fig. 4a). Detection accuracy also varies across the life course (Supplementary Fig. 4b). The model performs best when anomalous events are inserted before age 20 (97%), and dips modestly during the 20–30 range (93%).

The reordering task requires sorting a completely shuffled list of life events into chronological order without access to any timestamps: the model must rely entirely on its learned understanding of

which events logically precede others. Across 13,119 trajectories averaging 16.8 events in length, LifeSentence achieves a mean Kendall's Tau⁵⁷ of 91.2%, meaning that the model places two random events in the correct relative order over 90% of the time. The longest common subsequence⁵⁸ with the ground truth spans 79.3% of the trajectory on average, indicating that the order of roughly four-fifths of the biography is recoverable without access to any temporal information.

Together, these results indicate that LifeSentence has acquired an internal representation of which life events belong together and in what order they unfold. We next asked how LifeSentence responds when biographical information is incomplete, and whether systematic removal of events could reveal which ones carry the most structural weight. We evaluated all models on next-event prediction under three masking conditions of increasing severity: replacing individual events with explicit mask tokens, silently deleting events without markers, and redacting contiguous multi-year windows from the history.^{59–61} LifeSentence maintains the highest accuracy across all three conditions (Supplementary Table 4).

Beyond aggregate robustness, these masking experiments reveal which events carry the most structural weight. If the model has genuinely learned which events belong together and in what order, then removing structurally important events should degrade its predictions more than removing peripheral ones.⁶² We tested this by measuring the change in next-event prediction performance by type and timing of the masked event (Fig. 4).

Masking events in the 20–25 age range produces the largest accuracy degradation, consistent with this period's role as a critical developmental period^{43,44,45,[Roberts]}. The specific type of missing information disproportionately affects predictive capability: masking anchor events like military service^{63,64} start causes the highest degradation, confirming that these institutionally structured transitions serve as biographical anchors that constrain the space of possible futures.

We then tasked the model with imputing silently deleted events: LifeSentence achieves 83.0% accuracy for event-type identification, and mean placement error of 3.5 years. Highly structured events (military service completion, education completion) are recovered at rates above 0.95, while high-entropy transitions such as relationship status changes prove difficult to impute (Supplementary Fig. 10). The pattern mirrors the masking results: institutional events are both tightly constrained by their surrounding context, making them recoverable when absent, and serve as high-information structural pivots whose removal most disrupts downstream prediction.

LifeSentence recovers known stratification patterns from event sequences

Life events often co-occur with continuous outcomes central to social science: income, occupational prestige, health, and life satisfaction.^{65–67} We trained LifeSentence on a state imputation task in which the model receives an individual's discrete event trajectory, demographics (age and gender), and must recover associated continuous measurements. Crucially, the model receives no explicit supervision linking specific covariates to specific outcomes: no encoded rule that men should earn more, that college graduates should show steeper earnings growth, or that childbirth should affect mothers' income differently from fathers'.

Despite this, generated income trajectories recover known sociodemographic stratification patterns. When stratified by education (Fig. 5a), college-educated individuals show steeper income growth^{30,31} that accelerates through the 30s and 40s, while those without college education plateau earlier and at lower levels. The education premium in the model's predictions widens with

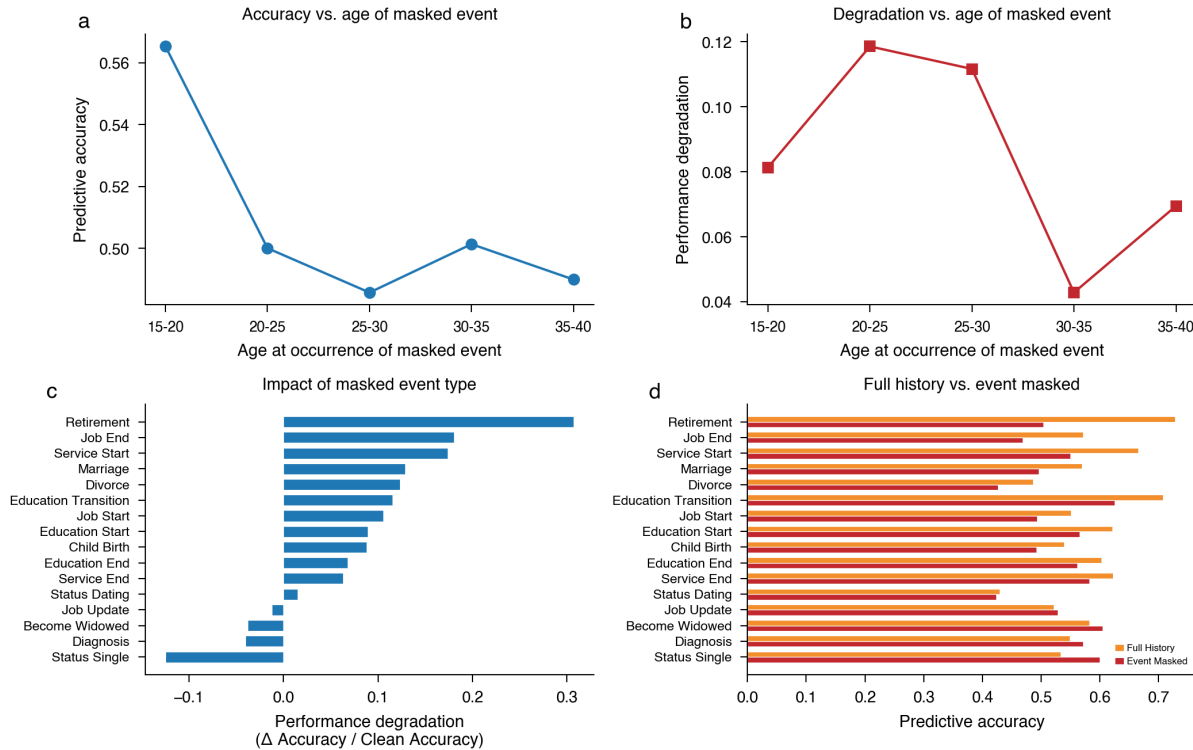


Figure 4— Sensitivity of predictive accuracy to masking of historical events. (a) Predictive accuracy on the next-event task as a function of the age at which historical events are masked. Accuracy is highest when events before age 20 are masked and drops to its lowest at ages 25–30, indicating that events during this period carry the most predictive information about an individual's future trajectory. (b) The same pattern expressed as relative performance degradation (change in accuracy normalised by clean-history accuracy). Degradation peaks at ages 20–25 (11.9%). (c) Performance degradation by masked event type, showing the normalised accuracy drop when each event type is removed from the history. Masking retirement produces the largest degradation (~ 0.30), followed by job end (~ 0.22), service start (~ 0.20), and marriage (~ 0.18), confirming that institutionally anchored transitions serve as high-information structural pivots. (d) Absolute predictive accuracy with full history (orange) versus with the event masked (red). The gap between bars visualises the informational contribution of each event type.

age, consistent with the theory of cumulative advantage, in which early educational investments compound into progressively larger income differentials over the career. A similar pattern emerges when stratifying by gender^{32,33} (Supplementary Fig. 11).

The model also recovers event-specific perturbations reflecting known structural inequalities. Income trajectories anchored to childbirth (Fig. 5b) reveal an asymmetry: male income continues rising uninterrupted after childbirth, while female income drops sharply at the moment of birth and recovers only slowly over the subsequent decade, never fully closing the pre-birth gap. LifeSentence reproduces this "motherhood penalty,"^{34,35} capturing both the immediate post-birth decline for women and the continued growth for men, despite never being trained with any explicit representation of gendered caregiving norms or labor market discrimination. For subjective well-being, the model captures how diagnosis events produce immediate declines in both life satisfaction and health satisfaction,^{68,69} tracking the slope and temporal dynamics of these perturbations (Supplementary Fig. 11b).

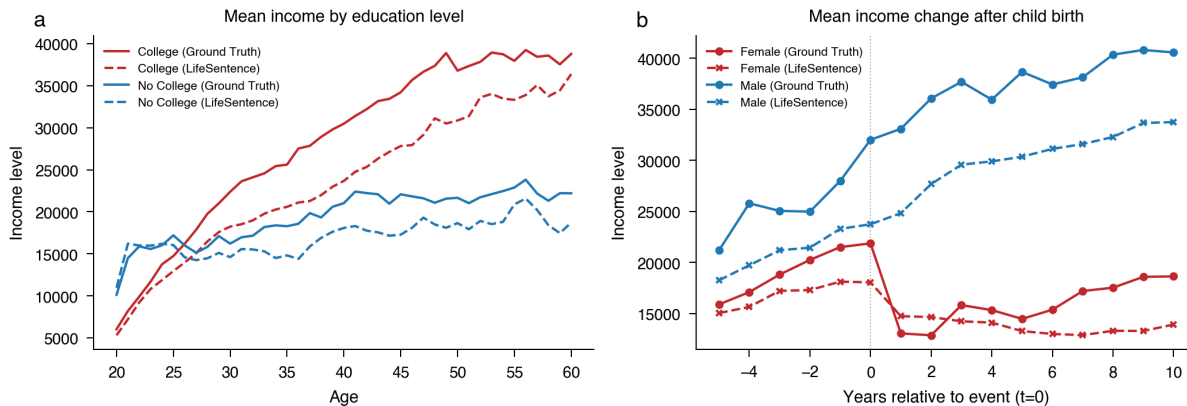


Figure 5 — Sociodemographic stratification of income trajectories. (a) Mean predicted income level across the lifespan stratified by education level, comparing college-educated (red) and non-college-educated (blue) individuals. LifeSentence predictions (dashed lines) recover the education premium without explicit supervision: college-educated trajectories show steeper growth that accelerates through the 30s and 40s, with the gap widening with age. (b) Mean income level in the years surrounding the birth of a child ($t = 0$, dotted vertical line) stratified by gender, comparing male (red) and female (blue) individuals. The model recovers the "motherhood penalty": male income continues to rise uninterrupted after childbirth, while female income drops at birth and recovers only slowly over the subsequent decade. Neither pattern was explicitly supervised (the model was never provided rules linking education to earnings growth or parenthood to gendered income divergence), suggesting that discrete event sequences carry information about associated continuous outcomes.

Through exposure to the statistical co-occurrence of discrete event sequences and continuous measurements across tens of thousands of individuals, the model has learned that the biographical signatures associated with gender, education, and parenthood systematically co-vary with particular income and well-being trajectories. In effect, the model’s learned representations capture statistical associations between event-sequence features and continuous outcomes that parallel documented patterns of cumulative advantage, without these associations having been specified as supervision targets.

Discussion

LifeSentence demonstrates that pretrained language models can compensate for smaller sample size in life-course prediction tasks.^{26,27,61,70,71} By encoding life events as natural-language descriptions, we supplement a panel dataset with distributional knowledge about education, employment, health, and mortality acquired from trillions of tokens of pretraining data.^{72,73} The pretrained model already encodes information about these concepts, while fine-tuning on rich biographical panel data then teaches the model how these concepts interact across a life: how an early educational decision shapes a career trajectory decades later, or how a health event restructures the timing of retirement. The division of labor from pretraining and fine-tuning reduces the sample size needed for competitive performance. A from-scratch transformer trained on the same 65,000 individuals must learn both concept semantics and biographical structure simultaneously. The pretrained model’s distributional representations provide a useful initialization, and fine-tuning⁷⁴ need only adapt these representations to life-course prediction and reasoning.

Beyond prediction, our results demonstrate that LifeSentence has acquired structured representations of biographical logic. The anomaly detection and reordering results demonstrate that LifeSentence has internalized which events belong within a single biography and in what order they unfold. The state imputation results go further, recovering the education premium, gender income gap, and motherhood penalty without explicit supervision. The masking experiments further reveal that this information is not uniformly distributed: events during the 20–30 age transition and institutionally anchored milestones carry more predictive weight, a finding potentially relevant to longitudinal study design.

The natural-language interface extends the range of expressible tasks. Prior architectures require task-specific output heads; LifeSentence accepts free-text instructions, enabling constrained-generation queries that would otherwise require bespoke model modifications. LifeSentence's capacity to interpret such instructions extends the model from a prediction engine into an interactive research tool.

Several limitations warrant consideration. First, LifeSentence was trained exclusively on a single panel study. Whether learned representations transfer to societies^{75,76} with fundamentally different institutional arrangements is an open question. Second, the current 20-category event vocabulary compresses human experience; major domains such as residential mobility⁷⁷ and criminal justice⁷⁸ involvement are absent. Third, the 24-billion-parameter model requires 4-bit quantization for feasible fine-tuning, representing a meaningful infrastructure barrier. Future work should explore whether smaller models⁷⁹ retain semantic transfer advantages. Fourth, LifeSentence does not provide calibrated uncertainty estimates. The model generates single trajectories rather than distributions over possible futures, yet human lives are fundamentally stochastic. Developing uncertainty quantification^{80–82} is critical before any individual-level application. Finally, the pretrained language model's semantic priors encode societal biases from its training corpus. When LifeSentence recovers the gender income gap, it is unclear to what extent these patterns reflect empirical regularities in the data versus stereotypical associations inherited from pretraining.^{83–85}

These results indicate that instruction-tuning a pretrained language model on structured biographical sequences can yield competitive life-course prediction from panel-scale samples and point toward further integration of distributional semantics with longitudinal social science data.

Methods

Ethics and Data Access

The data analysis was conducted using the German Socio-Economic Panel (SOEP),^{36,37} a representative longitudinal household survey administered by the German Institute for Economic Research (DIW Berlin). Access is granted exclusively for scientific purposes and is subject to strict confidentiality requirements that prohibit the identification of individual respondents or the transmission of microdata to unauthorized third parties. All model training and inference were performed locally on university-managed infrastructure; no individual-level data were transmitted to external APIs, cloud services, or third-party model providers. The base language model (Mistral Small 3.1) is an open-weight model whose parameters were downloaded and fine-tuned entirely on-premises, ensuring that SOEP microdata never left the secure research environment. Our model is a research prototype intended for scientific investigation of life trajectory predictability: before

any deployment in applied contexts such as policy planning or individual-level decision support, more comprehensive auditing would be required to evaluate demographic fairness across protected characteristics and to ensure appropriate transparency regarding model limitations.

Dataset

We constructed life-sequences from v37 of SOEP (1984-2020). The SOEP records contains detailed information across multiple life domains for each respondent, updated annually. We drew on five SOEP source files: the biography module (biobirth, bioedu, biomarsy), the spell data module (pbiospe), the individual questionnaire (pl, pkal), the individual-level cross-national equivalent file (pequiv), and the person-level tracking file (ppath, pgen), to assemble a comprehensive record of each individual's life trajectory.

We applied the following inclusion criteria: individuals must have valid demographic attributes (sex coded as male or female, and a positive birth year) and possess at least 10 discrete life events across the observation period. The resulting filtered dataset contained 65,606 individuals. These individuals were randomly partitioned into training (80%, $n = 52,485$) and test (20%, $n = 13,121$) sets at the individual level, ensuring that no person appeared in both partitions and that all tasks for a given individual were assigned entirely to one partition.

Employment data

Employment records were extracted from the SOEP activity spell file (pbiospe), which documents every discrete spell of biographical activity for each respondent. Each spell is classified into one of ten categories: school or college attendance, apprenticeship or vocational training, military or community service, full-time employment, part-time employment, unemployment, homemaker status, pensioner status, short-time work, and observational gaps. For each spell, the dataset records the start year and end year, yielding two events per spell (entry and exit). Employment spells were further enriched with occupational information from two additional sources. The biojob file provided occupational classifications encoded via the International Standard Classification of Occupations (ISCO-88), a hierarchical system that represents job types with four-digit codes (for example, code 2111 references "Physicists and Astronomers" and code 5141 references "Hairdressers"). The pgen file provided the Standard International Occupational Prestige Scale (SIOPS), a continuous index ranging from 6 to 78 that we discretized into five ordinal categories: very low autonomy and unskilled work (6–32), low autonomy and simple tasks (33–41), limited autonomy and intermediate complexity (42–50), dependent or independent positions of moderate prestige (51–63), and high-autonomy managerial positions (64+). Positional seniority information from pgen further classified each employment record by occupational rank (for example, unskilled worker, skilled worker, civil servant, or self-employed). Retirement events were identified from the calendar module (pkal) by flagging the first year in which a respondent reported receiving a pension; individuals without an early retirement record were assigned a statutory retirement event at age 67.

Education data

Education records were derived from the SOEP biography education module (bioedu), which documents the full educational trajectory of each respondent through nine milestone events: first and last attendance at early childhood education and care, primary school enrollment, transition to secondary school, exit from secondary school, entry into vocational training, exit from vocational training, entry into tertiary education, and exit from tertiary education. Each milestone records the calendar year and, where applicable, the institution type and certificate obtained. Vocational training types include apprenticeship, specialized vocational school, health care school, specialized technical school, and civil service training. Exit certificates include secondary school degrees (secondary, intermediate, technical, upper secondary, and dropout), vocational certificates (apprenticeship, vocational school, technical school, civil service, and dropout), and tertiary degrees (university of applied sciences, university, doctorate, and dropout).

Family data

Family records were assembled from the biography marriage and cohabitation spell file (biomarsy) and the biography birth file (biobirth). The marriage spell file documents each period of a respondent's relationship status, with spell types including: single, married, divorced, widowed, divorced or widowed (unspecified), married but separated, and living in a registered same-sex partnership. As with employment spells, each relationship spell generates two events (start and end of the spell). The birth file records the birth years of up to six children per respondent, yielding child-birth events with birth-order information (first child, second child, and so on).

Health data

Health records were drawn from the individual-level cross-national equivalent file (pequiv), which contains annual self-reported health information. We extracted 19 binary health indicators spanning three categories. Diagnostic conditions included stroke, hypertension, diabetes, cancer, psychiatric problems, arthritis, angina or heart conditions, and asthma or breathing difficulties (8 indicators). Functional limitations included difficulty climbing stairs, bathing, dressing, getting out of bed, shopping, walking, doing housework, and bending or lifting, as well as a general indicator that health limits vigorous physical activities (9 indicators). A hospitalization indicator recorded whether an accident required hospitalization, and a disability indicator recorded whether the respondent had become disabled. Mortality information was extracted from the person-level tracking file (ppath), which records the year of death for deceased respondents.

State variables

In addition to discrete life events, we recorded four continuous state variables measured annually: individual gross income (from pequiv), overall life satisfaction (from pequiv, on a 0–10 scale), health satisfaction (from pequiv, on a 0–10 scale), and occupational prestige (SIOPS score from pgen, discretized into five ordinal categories as described above). Unlike discrete events, these variables represent periodic measurements that characterize an individual's circumstances at particular time points. Negative or missing values were set to missing prior to analysis. Income values were retained as continuous measurements.

Sequence Construction and Preprocessing

From each appropriate SOEP source file, events were assigned one of the following 20 discrete event types:

JOB_START	EDUCATION_START	CHILD_BIRTH	BECOME_WIDOWED
JOB_END	EDUCATION_END	MARRIAGE	STATUS_SINGLE
JOB_UPDATE	EDUCATION_TRANSITION	DIVORCE	STATUS_DATING
RETIREMENT	SERVICE_START	SEPARATION	PARTNER_ABROAD
DIAGNOSIS	SERVICE_END	REMARRIAGE	DEATH

Each event carries associated detail fields specific to its domain (for example, occupation name, education level, diagnosis, or child birth order), the individual's age at the time of the event, and the calendar year.

We applied several refinement procedures to the raw event sequences. First, sequential medical diagnoses occurring within the same calendar year were aggregated into a single DIAGNOSIS event containing a deduplicated list of conditions, reducing redundancy while preserving diagnostic information. Second, employment events were contextualized based on persistent employment status: a JOB_START event occurring while an individual was already in continuous employment (full-time or part-time) was reclassified as JOB_UPDATE to distinguish between initial labor market entry and job changes within an unbroken employment spell. Third, within each calendar year, events were sorted so that DEATH always appeared last, ensuring that the temporal ordering of within-year events respected logical constraints. Finally, consecutive duplicate entries were suppressed: for example, if a respondent's relationship status in year t was identical to the status already recorded in the most recent prior year, the redundant entry was removed.

Event representation

Each life event was represented not as a categorical index but as a structured natural-language record. Employment events included occupation names drawn from ISCO-88 descriptors (for example, "Mechanical Engineers," "Secretaries"), positional seniority labels, and employment type. Education events included institution names (for example, "Upper secondary school"), certificate types, and educational levels drawn from the German system's standard terminology. Health events included diagnostic condition names. Family events included relationship status labels and child birth order.

Prompt template design

Each JSONL training example was converted into a structured natural-language prompt for supervised fine-tuning of the language model. Specific details of prompt formatting and layout are detailed in the Supplementary Information.

Task Formulation

A single prediction task cannot determine whether a model has genuinely learned the structure of human life trajectories or is merely exploiting surface-level correlations. To enable comprehensive evaluation, we formulated an 18-task taxonomy organized into three families of increasing inferential demand, each targeting a different dimension of model capability. Forecasting tasks assess whether the model can accurately predict future events at varying horizons, from single next-event prediction to complete remaining-life trajectory generation. Robustness tasks test whether predictions remain reliable when biographical information is incomplete, simulating the missing data conditions common in longitudinal panel studies. Reasoning tasks probe whether the model has acquired genuine structural understanding of biographical logic (such as the ability to detect anomalous events, recover chronological order without timestamps, and translate discrete event sequences into the continuous socioeconomic trajectories they produce). Together, these three families evaluate not only predictive accuracy but also the model’s capacity to internalize meaningful biographical structure. The 18-task taxonomy comprises the following categories:

Forecasting tasks.

- **NEXT_EVENT**: given a prefix of the event history and the corresponding state history, predict the immediate next discrete life event; this task was generated exhaustively using a sliding window over the entire trajectory, producing one example for every valid split point.
- **NEXT_3_EVENTS**: predict the next three events in chronological order.
- **PREDICT_UNTIL_EVENT**: predict all future events up to and including the next occurrence of a specified event.
- **ENTIRE_TRAJECTORY**: predict the complete remaining life trajectory from the current point.
- **PREDICT_UP_TO_YEAR**: predict all events occurring up to a specified future year.
- **SNAPSHOT_YEAR**: predict the specific events occurring in a randomly selected future year.
- **NEXT_SPECIFIC_TYPE**: predict the details of the next occurrence of a target event type.

Robustness tasks. These tasks tested model resilience to incomplete information.

- **MASKED_HISTORY_PREDICT_FUTURE** and **MASKED_HISTORY_PREDICT_NEXT_EVENT**: up to two events in the history were replaced with explicit [MASKED EVENT] tokens, and the corresponding state history entries for those years were removed.
- **IMPLICIT_GAP_PREDICT_FUTURE** and **IMPLICIT_GAP_PREDICT_NEXT_EVENT**: up to two events were silently removed from the history without any mask token, and state entries for the affected years were also removed.
- **MASKED_PERIOD_PREDICT_FUTURE** and **MASKED_PERIOD_PREDICT_NEXT_EVENT**: a contiguous block of 5–10 years was redacted from the history, with all events in that range replaced by a descriptive mask token indicating the redacted period, and state entries within that range removed.

Reasoning tasks.

- **CONNECT_POINTS**: given the history up to approximately age 25 and a single target event at approximately age 65 (along with state history up to the start point), generate the plausible sequence of events connecting these two points.
- **IMPLICIT_REMOVAL**: given a timeline with one silently removed event, identify the missing event and its correct position.
- **ANOMALY_DETECTION**: given a timeline with one injected distractor event (sampled from the training event pool with temporally consistent age and year interpolation), identify the anomalous event.
- **STATE_IMPUTATION**: given the discrete event history alone (no state variables), estimate the full continuous state history.
- **REORDERING**: given a shuffled set of events with age and year fields removed, reconstruct the correct chronological order.

All tasks except **NEXT_EVENT** were generated at up to three randomly sampled split points per individual to control dataset size, while **NEXT_EVENT** was generated exhaustively at every valid split point. The **CONNECT_POINTS**, **IMPLICIT_REMOVAL**, **ANOMALY_DETECTION**, **STATE_IMPUTATION** and **REORDERING** tasks were each generated once per individual from the full trajectory.

Model Architecture

LifeSentence: Large Language Model Approach

Our primary model, LifeSentence, adapts a pretrained large language model to life trajectory prediction through supervised fine-tuning. We employ Low-Rank Adaptation (LoRA)⁴⁰ to enable efficient parameter-efficient training while preserving the pretrained model's capabilities. Each training example was converted into the natural-language prompt format described (see Supplementary Information *Sequence Construction and Preprocessing*), and the fine-tuned model was trained to produce the corresponding JSON target via supervised next-token prediction.

Model architecture and training. We fine-tuned Mistral Small 3.1 24B Base (unsloth/Mistral-Small-3.1-24B-Base-2503), a 24-billion-parameter decoder-only language model, using the Unsloth library for efficient training and inference. Full finetuning of a 24B-parameter model exceeds available GPU memory; we therefore adopt the QLoRA⁸⁶ framework, where the frozen base model weights were stored in 4-bit NormalFloat quantization, while the trainable adapter parameters and all gradient computations used bfloat16 precision throughout. Low-Rank Adaptation (LoRA) was applied with rank $r=16$ and $\alpha=16$ (effective scaling factor of 1.0), targeting all attention and feed-forward projection matrices. No dropout was applied to the LoRA layers, and no bias terms were trained.

Training was conducted for 1 epoch on a single NVIDIA A100 with the following hyperparameters: learning rate of 2×10^{-5} ; paged AdamW optimizer (32-bit);⁸⁷ linear learning-rate scheduler with a 3% warmup ratio;⁸⁸ per-device batch size of 8; gradient accumulation over 4 steps (effective batch size of 32);⁸⁹ maximum gradient norm of 0.3.

Inference and evaluation. At inference time, the fine-tuned model was loaded from the saved checkpoint in 4-bit quantization using Unsloth’s FastLanguageModel and placed in inference mode. Prompts were constructed identically to training using the same formatting functions. All predictions were generated using greedy decoding (temperature = 0). Model outputs were parsed by locating the outermost pair of curly braces in the generated text and attempting JSON deserialization of the enclosed substring. Outputs that failed to parse were retained in the evaluation dataset and scored as incorrect predictions across all metrics; no outputs were excluded from reported results.

Benchmark Models

We benchmarked LifeSentence against two classes of baseline models that represent the dominant approaches in the life-course prediction literature. Classical machine learning models (logistic regression and XGBoost) operate on hand-engineered fixed-length feature vectors extracted from the event history, discarding sequential ordering but providing strong baselines on tabular prediction tasks. Deep learning models (Transformer encoder, LSTM, and GRU) receive the raw event sequence as input and can in principle learn temporal dependencies directly from data, but must learn both event semantics and sequential structure from scratch using only the panel data. This two-class design allows us to disentangle the contributions of sequential modeling (deep learning vs. classical) from the contribution of pretrained semantic knowledge (LifeSentence vs. all baselines). All baselines were trained and evaluated on the same data partitions and task definitions as LifeSentence.

Classical machine learning baselines

Feature extraction. All classical baselines shared a common feature extraction pipeline. For each example, a fixed-length feature vector was computed from the event history, state history and demographic information. Demographic features comprised binary indicators for gender, normalized birth year, and normalized birth decade. Event count features included, for each of the 20 event types, the total count and a binary has-occurred indicator, and for each of the 5 event domains (family, education, employment, health, service), the total domain count. Temporal features comprised normalized current age, minimum observed age, age span, total number of events (raw and log-transformed), year span, latest observed year and one-hot encoded age bins (0–18, 18–25, 25–35, 35–45, 45–55, 55–65, 65–100). Last-event features included one-hot encoding of the most recent event’s type and domain, normalized age of the last event and time elapsed since the last event. Bigram features captured transition patterns via one-hot encoding of the second-to-last event type. State features comprised the most recent income (normalized by dividing by 100,000, plus log-transformed), life satisfaction score and health satisfaction score (each normalized to 0–1 by dividing by 10). Recent context features captured the proportional frequency of each event type within the last 5 events. All features were standardized using a StandardScaler fitted on the training set; NaN and infinite values were replaced with zero prior to scaling.

Task categorization. The multi-task evaluation set was partitioned into three categories with respect to classical model capabilities. Single-event prediction tasks (NEXT_EVENT, MASKED_HISTORY_PREDICT_NEXT_EVENT, IMPLICIT_GAP_PREDICT_NEXT_EVENT, MASKED_PERIOD_PREDICT_NEXT_EVENT) were evaluated directly. Sequence generation tasks (NEXT_3_EVENTS, PREDICT_UNTIL_EVENT, ENTIRE_TRAJECTORY,

PREDICT_UP_TO_YEAR, and their masked/corrupted variants) were handled through autoregressive rollout. Seven task types (NEXT_SPECIFIC_TYPE, SNAPSHOT_YEAR, CONNECT_POINTS, IMPLICIT_REMOVAL, ANOMALY_DETECTION, REORDERING, STATE_IMPUTATION) were deemed unsupported because they required capabilities beyond point prediction and were excluded from classical model evaluation.

XGBoost. The XGBoost⁹⁰ baseline employed two models: an XGBClassifier for event type prediction and an XGBRegressor for event age prediction. The classifier was configured with the multi:softmax objective, 100 estimators, maximum depth 6, learning rate 0.1, and histogram-based tree construction. The regressor used 100 estimators, maximum depth 5 and learning rate 0.1, and was trained only on examples with valid target ages. We trained on all single-event prediction tasks including masked and corrupted variants, and “all” (every task yielding a valid target event type). For sequence generation tasks, the model was applied autoregressively: after predicting the next event type and age, a synthetic event dictionary was appended to the running history, features were re-extracted from the updated history, and the next prediction was generated. Stopping criteria included death prediction, reaching a specified target year or reaching a task-specific maximum sequence length (3 for NEXT_3_EVENTS, 30 for bounded tasks, 50 for full trajectory prediction).

Logistic regression. The logistic regression baseline followed an identical pipeline to XGBoost, substituting the tree-based models with linear models. A multinomial logistic regression classifier (L-BFGS solver, maximum 1,000 iterations) was used for event type prediction, and a standard linear regression model was used for age prediction. Both models used the same StandardScaler and feature extraction pipeline. The same training mode, autoregressive sequence generation procedure and stopping criteria as XGBoost were employed.

Deep learning models

Three deep learning models—a Transformer encoder,¹⁷ an LSTM⁹¹ and a GRU⁹²—shared a common base architecture. The input representation consisted of four fused embedding components, summed element-wise: (1) a learned event-type embedding of dimension $d = 256$ for each token in the vocabulary (20 event types plus 4 special tokens: <PAD>, <SOS>, <EOS>, <UNK>); (2) a linear projection of the normalized age (age/100) to d dimensions; (3) a learned gender embedding broadcast across the sequence length; and (4) a linear projection of the normalized birth year ((birth_year - 1900)/100) broadcast across the sequence. These four components were passed through a dropout layer (rate 0.1) to produce the fused input representation. Each model produced two outputs from the final hidden state: event type logits via a linear classification head mapping d to the vocabulary size, and a normalized predicted age via a single-output linear regression head. The training objective combined cross-entropy loss for event type classification with mean squared error loss for age prediction.

Transformer. The Transformer model used three TransformerEncoderLayers with $d = 256$, 4 attention heads and dropout rate 0.1. The prediction was derived from the hidden state of the last valid (non-padding) token in each sequence. Positional encoding as well as a causal mask are applied. Training used the Adam optimizer with a learning rate of 1×10^{-3} , batch size 128 and up to 30 training epochs, with early stopping after 15 epochs.⁹³

LSTM and GRU. The LSTM and GRU models used the same input fusion and output heads. The LSTM employed a three-layer LSTM with hidden dimension 256. The GRU used an identically

configured three-layer GRU. Both models leveraged PyTorch’s efficient handling of variable-length inputs, using the padding mask to compute true sequence lengths. The final hidden state (h_n) was used as the summary vector for prediction. Training used the Adam optimizer with learning rate 1×10^{-3} , batch size 128 and up to 30 training epochs, with early stopping after 15 epochs.

Inference. At test time, all three neural models used greedy decoding: the event type with the highest logit was selected, and the predicted normalized age was rescaled (multiplied by 100) and clamped to be at least 0.5 greater than the last observed age to enforce monotonicity. For sequence generation tasks, predictions were generated autoregressively by appending each predicted event to the running history and re-encoding the updated sequence, up to task-specific maximum step counts (1 for single-event tasks, 3 for NEXT_3_EVENTS, 30 for other sequence tasks). Generation terminated upon predicting DEATH, <EOS>, <PAD> or exceeding age 100.

Evaluation Metrics

We employed a list of metrics to assess model performance across the 18-task taxonomy, as no single metric captures all dimensions of life-course prediction. Each metric is designed to evaluate a specific aspect of model capability. Event-level classification metrics (Event Type Accuracy, Joint Accuracy, Conditional MAE) assess single-event forecasting performance and are the primary measures for prediction tasks. Sequence-level trajectory metrics (Jaccard Similarity, Multiset Jaccard, Levenshtein Distance, Wasserstein Distance) evaluate the structural and temporal fidelity of generated multi-event trajectories, serving as the primary measures for trajectory generation and constrained generation tasks. Specialised classification metrics (Anomaly Detection Accuracy, Imputation Accuracy) and ordering metrics (Kendall’s τ , Longest Common Subsequence) evaluate the reasoning tasks that probe whether the model has acquired genuine structural understanding of biographical logic. Finally, constraint satisfaction measures assess whether generated trajectories comply with task-specific requirements, providing a complementary evaluation of the model’s ability to follow natural-language instructions. Metrics are organised below by these categories; full results are reported in the corresponding tables and figures.

Event-level classification metrics. Event Type Accuracy measures the proportion of predictions where the predicted event type matches the ground truth. Joint Accuracy requires both a correct event type and a predicted age to be correct (after rounding). Conditional Mean Absolute Error (Conditional MAE) reports the mean absolute age error in years, computed only over predictions where the event type was correctly identified. These metrics are reported for single-event tasks (Table 1, Supplementary Fig. 1, Supplementary Fig. 2) and for the next-three-events task (Supplementary Table 3a), where they are computed independently per slot and averaged across positions.

Specialised classification metrics. Anomaly Detection Accuracy measures the proportion of trajectories in which the model correctly identifies an injected distractor event (Supplementary Fig. 4). Imputation Accuracy measures the proportion of silently deleted events whose type is correctly recovered from surrounding context; Placement Accuracy further requires that the recovered event be assigned to the correct temporal position (Supplementary Fig. 10).

Sequence-level trajectory metrics. For trajectory generation tasks, we report four complementary metrics. Jaccard Similarity⁴⁸ measures the set overlap between predicted and

ground-truth unique event types. Multiset Jaccard⁵¹ extends this to account for event-type frequency (e.g., penalising a trajectory that predicts two childbirths when three occurred). Levenshtein Distance⁴⁹ measures the minimum number of insertions, deletions, and substitutions required to transform the predicted event-type sequence into the ground truth. Wasserstein Distance⁵⁰ measures the optimal transport cost of moving predicted event ages to their ground-truth temporal positions. These are reported in Supplementary Table 2 (unconstrained generation) and Supplementary Table 3b (constrained generation).

Constraint satisfaction. For the PREDICT_UNTIL_EVENT task, Constraint Satisfaction Rate measures the proportion of generated trajectories that actually terminate at the requested milestone event (Supplementary Table 3b).

Ordering and structural metrics. For the reordering task, we report Kendall's τ ⁵⁷, which measures the proportion of concordant event pairs between predicted and true orderings, and Longest Common Subsequence⁵⁸ proportion, which captures the fraction of the trajectory recovered as an unbroken in-order chain. Transition probability error quantifies the absolute difference between the model's predicted pairwise event-transition probabilities and ground-truth transition matrices (Supplementary Fig. 3).

Data availability

The data used in this study are not publicly available due to German Data Protection laws. Access to the data can be obtained via the German Institute for Economic Research (DIW).

Code availability

The source code for the data pre-processing, model training, analysis and visualization is available on GitHub at <https://github.com/samuelliu2019/life-sentence>.

References

1. Vaillant, G. E. & Mukamal, K. Successful aging. *Am. J. Psychiatry* 158, 839–847 (2001).
2. Diener, E. & Seligman, M. E. P. Very happy people. *Psychol. Sci.* 13, 81–84 (2002).
3. Moffitt, T. E. et al. A gradient of childhood self-control predicts health, wealth, and public safety. *Proc. Natl Acad. Sci. USA* 108, 2693–2698 (2011).
4. Salganik, M. J. et al. Measuring the predictability of life outcomes with a scientific mass collaboration. *Proc. Natl Acad. Sci. USA* 117, 8398–8403 (2020).
5. Grossmann, I. et al. Insights into the accuracy of social scientists' forecasts of societal change. *Nat. Hum. Behav.* 7, 484–501 (2023).
6. Oparina, E. et al. Machine learning in the prediction of human wellbeing. *Sci. Rep.* 15, 1632 (2025).
7. Halpern-Manners, A., Warren, J. R., Raymo, J. M. & Nicholson, D. A. The impact of work and family life histories on economic well-being at older ages. *Social Forces* 93, 1369–1396 (2015).
8. Wills, A. K. et al. Life course trajectories of systolic blood pressure using longitudinal data from eight UK cohorts. *PLoS Medicine* 8, e1000440 (2011).
9. Hayward, M. D. & Gorman, B. K. The long arm of childhood: the influence of early-life social conditions on men's mortality. *Demography* 41, 87–107 (2004).
10. Ferraro, K. F., Schafer, M. H. & Wilkinson, L. R. Childhood disadvantage and health problems in middle and later life: early imprints on physical health? *American Sociological Review* 81, 107–133 (2016).
11. Willson, A. E., Shuey, K. M. & Elder, G. H. Jr. Cumulative advantage processes as mechanisms of inequality in life course health. *American Journal of Sociology* 112, 1886–1924 (2007).

12. Rook, K. S., Catalano, R. & Dooley, D. The timing of major life events: effects of departing from the social clock. *American Journal of Community Psychology* 17, 233–258 (1989).
13. Elder, G. H., Jr. The life course as developmental theory. *Child Dev.* 69, 1–12 (1998).
14. Elder, G. H., Jr. & Shanahan, M. J. The life course and human development. In *Handbook of Child Psychology* Vol. 1 (ed. Lerner, R. M.) 665–715 (Wiley, 2006).
15. Topel, R. H. & Ward, M. P. Job mobility and the careers of young men. *Q. J. Econ.* 107, 439–479 (1992).
16. Lynch, J. W., Kaplan, G. A. & Shema, S. J. Cumulative impact of sustained economic hardship on physical, cognitive, psychological, and social functioning. *N. Engl. J. Med.* 337, 1889–1895 (1997).
17. Vaswani, A. et al. Attention is all you need. In *Advances in Neural Information Processing Systems* 30 (NeurIPS) (2017).
18. Devlin, J., Chang, M.-W., Lee, K. & Toutanova, K. BERT: Pre-training of deep bidirectional transformers for language understanding. In *Proc. NAACL-HLT 2019*, 4171–4186 (2019).
19. Shmatko, A. et al. Learning the natural history of human disease with generative transformers. *Nature* 647, 248–256 (2025).
20. Renc, P. et al. Zero shot health trajectory prediction using transformer. *npj Digit. Med.* 7, 256 (2024).
21. Vafa, K., Palikot, E., Du, T., Kanodia, A., Athey, S. & Blei, D. M. CAREER: a foundation model for labor sequence data. Preprint at <https://arxiv.org/abs/2202.08370> (2024).
22. Savcisen, G. et al. Using sequences of life-events to predict human lives. *Nat. Comput. Sci.* 4, 43–56 (2024).
23. Yang, E., Li, M. D., Raghavan, S., Deng, F., Lang, M., Succi, M. D., Huang, A. J. & Kalpathy-Cramer, J. Transformer versus traditional natural language processing: how much data is enough for automated radiology report classification? *Br. J. Radiol.* 96, 20220769 (2023).
24. Grinsztajn, L., Oyallon, E. & Varoquaux, G. Why do tree-based models still outperform deep learning on typical tabular data? in *Advances in Neural Information Processing Systems* 35 (NeurIPS, 2022).
25. Raffel, C. et al. Exploring the limits of transfer learning with a unified text-to-text transfer transformer. *J. Mach. Learn. Res.* 21, 1–67 (2020).
26. Wei, J. et al. Finetuned language models are zero-shot learners. In *Proc. International Conference on Learning Representations* (2022).
27. Du, T., Kanodia, A., Brunborg, H., Vafa, K. & Athey, S. LABOR-LLM: language-based occupational representations with large language models. Preprint at <https://arxiv.org/abs/2406.17972> (2024).
28. Aribandi, V. et al. ExT5: towards extreme multi-task scaling for transfer learning. In *Proc. International Conference on Learning Representations* (2022).
29. Lundberg, I., Brown-Weinstock, R., Clampet-Lundquist, S., Pachman, S., Nelson, T. J., Yang, V., Edin, K. & Salganik, M. J. The origins of unpredictability in life outcome prediction tasks. *Proc. Natl Acad. Sci. USA* 121, e2322973121 (2024).
30. Tamborini, C. R., Kim, C. & Sakamoto, A. Education and lifetime earnings in the United States. *Demography* 52, 1383–1407 (2015).
31. Bhuller, M., Mogstad, M. & Salvanes, K. G. Life-cycle earnings, education premiums, and internal rates of return. *J. Labor Econ.* 35, 993–1030 (2017).
32. Bertrand, M., Goldin, C. & Katz, L. F. Dynamics of the gender gap for young professionals in the financial and corporate sectors. *Am. Econ. J. Appl. Econ.* 2, 228–255 (2010).
33. Barth, E., Kerr, S. P. & Olivetti, C. The dynamics of gender earnings differentials: evidence from establishment data. *Eur. Econ. Rev.* 134, 103713 (2021).
34. Kleven, H., Landais, C. & Sogaard, J. E. Children and gender inequality: evidence from Denmark. *Am. Econ. J. Appl. Econ.* 11, 181–209 (2019).
35. Almond, D., Cheng, Y. & Machado, C. Large motherhood penalties in US administrative microdata. *Proc. Natl Acad. Sci. USA* 120, e2209740120 (2023).
36. Goebel, J. et al. The German Socio-Economic Panel (SOEP). *Jahrb. Natl.ökon. Stat.* 239, 345–360 (2019).
37. Wagner, G. G., Frick, J. R. & Schupp, J. The German Socio-Economic Panel Study (SOEP) – scope, evolution and enhancements. *Schmollers Jahrb.* 127, 139–169 (2007).
38. Gurnee, W. & Tegmark, M. Language models represent space and time. In *Proc. International Conference on Learning Representations* (2024).
39. Aghajanyan, A., Gupta, S. & Zettlemoyer, L. Intrinsic dimensionality explains the effectiveness of language model fine-tuning. In *Proc. 59th Annual Meeting of the Association for Computational Linguistics* 7319–7328 (ACL, 2021).

40. Hu, E. J. et al. LoRA: low-rank adaptation of large language models. In Proc. 10th International Conference on Learning Representations <https://openreview.net/forum?id=nZeVKeeFYf9> (2022).
41. Shaw, C. et al. Comparison of imputation strategies for incomplete longitudinal data in life-course epidemiology. *Am. J. Epidemiol.* 192, 2075–2084 (2023).
42. Lazar, A., Jin, L., Spurlock, C. A., Wu, K., Sim, A. & Todd, A. Evaluating the effects of missing values and mixed data types on social sequence clustering using t-SNE visualization. *J. Data Inf. Qual.* 11, 7:1–7:22 (2019).
43. Rindfuss, R. R. The young adult years: diversity, structural change, and fertility. *Demography* 28, 493–512 (1991).
44. Manning, W. D. Young adulthood relationships in an era of uncertainty: a case for cohabitation. *Demography* 57, 799–819 (2020).
45. Eliason, S. R., Mortimer, J. T. & Vuolo, M. The transition to adulthood: life course structures and subjective perceptions. *Soc. Psychol. Q.* 78, 205–227 (2015).
46. Elzinga, C. H. Complexity of categorical time series. *Sociol. Methods Res.* 38, 463–481 (2010).
47. Van Winkle, Z. Family trajectories across time and space: increasing complexity in family life courses in Europe? *Demography* 55, 135–164 (2018).
48. Jaccard, P. The distribution of the flora in the alpine zone. *New Phytologist* 11, 37–50 (1912).
49. Levenshtein, V. I. Binary codes capable of correcting deletions, insertions, and reversals. *Sov. Phys. Dokl.* 10, 707–710 (1966).
50. Vaserstein, L. N. Markov processes over denumerable products of spaces, describing large systems of automata. *Probl. Peredachi Inf.* 5, 64–72 (1969).
51. Levandowsky, M. & Winter, D. Distance between sets. *Nature* 234, 34–35 (1971).
52. Begall, K. & Grunow, D. Labour force transitions around first childbirth in the Netherlands. *Eur. Sociol. Rev.* 31, 697–712 (2015).
53. Hallqvist, J., Lynch, J., Bartley, M., Lang, T. & Blane, D. Can we disentangle life course processes of accumulation, critical period and social mobility? An analysis of disadvantaged socio-economic positions and myocardial infarction in the Stockholm Heart Epidemiology Program. *Soc. Sci. Med.* 58, 1555–1562 (2004).
54. McCoy, R. T., Pavlick, E. & Linzen, T. Right for the wrong reasons: diagnosing syntactic heuristics in natural language inference. Proc. 57th Annu. Meet. Assoc. Comput. Linguist. 3428–3448 (2019).
55. Niven, T. & Kao, H.-Y. Probing neural network comprehension of natural language arguments. Proc. 57th Annu. Meet. Assoc. Comput. Linguist. 4658–4664 (2019).
56. Brückner, H. & Mayer, K. U. De-standardization of the life course: what it might mean? And if it means anything, whether it actually took place? *Adv. Life Course Res.* 9, 27–53 (2005).
57. Kendall, M. G. A new measure of rank correlation. *Biometrika* 30, 81–93 (1938).
58. Hirschberg, D. S. A linear space algorithm for computing maximal common subsequences. *Commun. ACM* 18, 341–343 (1975).
59. Petroni, F. et al. Language models as knowledge bases? In Proceedings of the 2019 Conference on Empirical Methods in Natural Language Processing and the 9th International Joint Conference on Natural Language Processing (EMNLP-IJCNLP) 2463–2473 (Association for Computational Linguistics, 2019).
60. Wu, Z., Chen, Y., Kao, B. & Liu, Q. Perturbed masking: parameter-free probing for analyzing and interpreting BERT. In Proceedings of the 58th Annual Meeting of the Association for Computational Linguistics 4166–4176 (Association for Computational Linguistics, 2020).
61. Talmor, A., Elazar, Y., Goldberg, Y. & Berant, J. oLMpics – on what language model pre-training captures. *Trans. Assoc. Comput. Linguist.* 8, 743–758 (2020).
62. Zeiler, M. D. & Fergus, R. Visualizing and understanding convolutional networks. In *Computer Vision – ECCV 2014* (eds Fleet, D. et al.) 818–833 (Springer, 2014).
63. Elder, G. H. Jr. Military times and turning points in men's lives. *Dev. Psychol.* 22, 233–245 (1986).
64. Sampson, R. J. & Laub, J. H. Socioeconomic achievement in the life course of disadvantaged men: military service as a turning point, circa 1940–1965. *Am. Sociol. Rev.* 61, 347–367 (1996).
65. Clark, A. E., Diener, E., Georgellis, Y. & Lucas, R. E. Lags and leads in life satisfaction: a test of the baseline hypothesis. *The Economic Journal* 118, F222–F243 (2008).
66. Jacobson, L. S., LaLonde, R. J. & Sullivan, D. G. Earnings losses of displaced workers. *American Economic Review* 83, 685–709 (1993).
67. Sullivan, D. & von Wachter, T. Job displacement and mortality: an analysis using administrative data. *The Quarterly Journal of Economics* 124, 1265–1306 (2009).
68. Stacherl, B. & Sauzet, O. Chronic disease onset and wellbeing development: longitudinal analysis and the role of healthcare access. *Eur. J. Public Health* 34, 29–34 (2024).

69. Stöckel, J., van Exel, J. & Brouwer, W. B. F. Adaptation in life satisfaction and self-assessed health to disability—evidence from the UK. *Soc. Sci. Med.* 328, 115996 (2023).
70. Gao, T., Fisch, A. & Chen, D. Making pre-trained language models better few-shot learners. In *Proceedings of the 59th Annual Meeting of the Association for Computational Linguistics and the 11th International Joint Conference on Natural Language Processing (ACL-IJCNLP)* 3816–3830 (Association for Computational Linguistics, 2021).
71. Roberts, A., Raffel, C. & Shazeer, N. How much knowledge can you pack into the parameters of a language model? In *Proceedings of the 2020 Conference on Empirical Methods in Natural Language Processing (EMNLP)* 5418–5426 (Association for Computational Linguistics, 2020).
72. Heggelmann, S., Buendia, A., Lang, H., Agrawal, M., Jiang, X. & Sontag, D. TabLLM: Few-shot Classification of Tabular Data with Large Language Models. *Proc. 26th International Conference on Artificial Intelligence and Statistics (AISTATS)* PMLR 206, 5549–5581 (2023).
73. Dinh, T., Zeng, Y., Zhang, R., Lin, Z., Gira, M., Rajput, S., Sohn, J., Papailiopoulos, D. & Lee, K. LIFT: Language-Interfaced Fine-Tuning for Non-Language Machine Learning Tasks. *Advances in Neural Information Processing Systems* 35, 11763–11784 (2022).
74. Howard, J. & Ruder, S. Universal Language Model Fine-tuning for Text Classification. *Proc. 56th Annual Meeting of the Association for Computational Linguistics* 1, 328–339 (2018).
75. Aisenbrey, S. & Fasang, A. E. The interplay of work and family trajectories over the life course: Germany and the United States in comparison. *Am. J. Sociol.* 122, 1448–1484 (2017).
76. Bratberg, E., Davis, J., Mazumder, B., Nybom, M., Schnitzlein, D. D. & Vaage, K. A comparison of intergenerational mobility curves in Germany, Norway, Sweden, and the US. *Scand. J. Econ.* 119, 72–101 (2017).
77. Stovel, K. & Bolan, M. Residential trajectories: using optimal alignment to reveal the structure of residential mobility. *Sociol. Methods Res.* 32, 559–598 (2004).
78. Massoglia, M. Incarceration as exposure: the prison, infectious disease, and other stress-related illnesses. *J. Health Soc. Behav.* 49, 56–71 (2008).
79. Hinton, G., Vinyals, O. & Dean, J. Distilling the knowledge in a neural network. Preprint at <https://arxiv.org/abs/1503.02531> (2015).
80. Guo, C., Pleiss, G., Sun, Y. & Weinberger, K. Q. On calibration of modern neural networks. In *Proceedings of the 34th International Conference on Machine Learning* 1321–1330 (PMLR, 2017).
81. Kuhn, L., Gal, Y. & Farquhar, S. Semantic uncertainty: linguistic invariances for uncertainty estimation in natural language generation. In *Proceedings of the 11th International Conference on Learning Representations (ICLR, 2023)*.
82. Romano, Y., Patterson, E. & Candès, E. J. Conformalized quantile regression. In *Advances in Neural Information Processing Systems* 32, 3538–3548 (NeurIPS, 2019).
83. Bolukbasi, T., Chang, K.-W., Zou, J. Y., Saligrama, V. & Kalai, A. T. Man is to computer programmer as woman is to homemaker? Debiasing word embeddings. In *Advances in Neural Information Processing Systems* 29, 4349–4357 (NeurIPS, 2016).
84. Caliskan, A., Bryson, J. J. & Narayanan, A. Semantics derived automatically from language corpora contain human-like biases. *Science* 356, 183–186 (2017).
85. Zhao, J., Wang, T., Yatskar, M., Ordonez, V. & Chang, K.-W. Gender bias in coreference resolution: evaluation and debiasing methods. In *Proceedings of the 2018 Conference of the North American Chapter of the Association for Computational Linguistics: Human Language Technologies Vol. 2*, 15–20 (ACL, 2018).
86. Dettmers, T., Pagnoni, A., Holtzman, A. & Zettlemoyer, L. QLoRA: Efficient Finetuning of Quantized LLMs. *Adv. Neural Inf. Process. Syst.* 36, 10088–10115 (2023).
87. Loshchilov, I. & Hutter, F. Decoupled weight decay regularization. in *International Conference on Learning Representations (ICLR, 2019)*.
88. Ma, J. & Yarats, D. On the adequacy of untuned warmup for adaptive optimization. *Proc. AAAI Conf. Artif. Intell.* 35, 8828–8836 (2021).
89. Smith, S. L., Kindermans, P.-J., Ying, C. & Le, Q. V. Don't decay the learning rate, increase the batch size. in *International Conference on Learning Representations (ICLR, 2018)*.
90. Chen, T. & Guestrin, C. XGBoost: a scalable tree boosting system. In *Proceedings of the 22nd ACM SIGKDD International Conference on Knowledge Discovery and Data Mining* 785–794 (ACM, 2016).
91. Hochreiter, S. & Schmidhuber, J. Long short-term memory. *Neural Comput.* 9, 1735–1780 (1997).
92. Cho, K. et al. Learning phrase representations using RNN encoder–decoder for statistical machine translation. In *Proceedings of the 2014 Conference on Empirical Methods in Natural Language Processing (EMNLP)* 1724–1734 (Association for Computational Linguistics, 2014).

93. Yao, Y., Rosasco, L. & Caponnetto, A. On early stopping in gradient descent learning. *Constr. Approx.* 26, 289–315 (2007).

Supplementary Information

*Language models can encode human life course trajectories
from longitudinal panel data*

Prompt template design

The prompt followed a fixed five-section template:

```
### System:
You are a Life Trajectory Specialist. You are trained to analyze
longitudinal life history data, including discrete events
(employment, family, health) and continuous state variables
(income, satisfaction), to perform complex forecasting and
reasoning tasks.

### Task Type:
{TASK_IDENTIFIER}

### Input Data:
{FORMATTED_INPUT}

### Instruction:
Subject: {gender}, Born: {birth_year}. {task_instruction}
Return the answer strictly as a valid JSON object.
Do not output any additional text, explanations, or markdown
formatting.

### Prediction:
{MODEL_OUTPUT}
```

The System section was identical across all tasks. The Task Type section contained one of the 18 task identifiers (for example, NEXT_EVENT, ANOMALY_DETECTION, REORDERING). The Instruction section embedded the individual's demographic information (gender and birth year) and the task-specific directive. The Prediction section contained the ground-truth JSON target during training, and was left empty at inference time for the model to complete via greedy decoding.

Discrete event formatting

Each life event was rendered as a single line of the form:

```
- Event: {EVENT_TYPE} at age {age} ({year}). Details: {json_details}
```

The event-detail dictionary was serialized as JSON with keys sorted alphabetically to ensure deterministic output. For example, a full-time employment event might be rendered as:

```
- Event: JOB_START at age 24 (1972). Details: {"employment_type":
  "Full-Time Employment", "occupation": "Mechanical Engineers",
  "position": "Skilled worker"}
```

Events without associated details (for example, DEATH or SEPARATION) omitted the Details suffix. Masked events were rendered as - [MASKED EVENT]: Event hidden for individually masked events, or - [MASKED EVENT]: Redacted Period (1985-1992) for contiguous temporal redactions.

State history formatting

Continuous state measurements were grouped by calendar year and consolidated into a single line per year. Within each line, state types were sorted alphabetically and formatted as human-readable key-value pairs. For example:

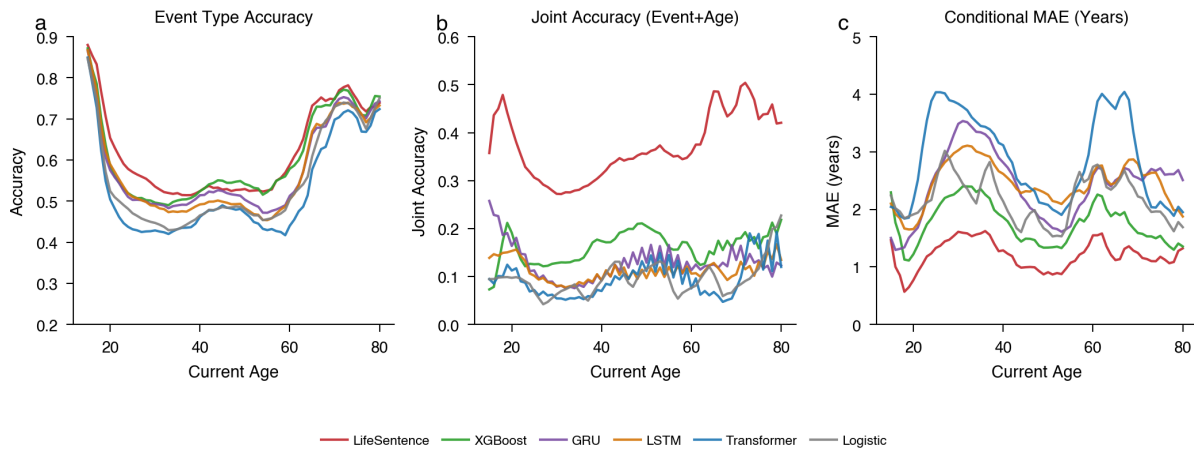
```
- At age 35 (1983): Health Satisfaction: 7, Income Level: 42850.0,  
  Job Prestige: 3: Limited autonomy of action, intermediate,  
  Life Satisfaction: 8
```

Years without any valid state measurements were omitted. If no state measurements were available for an individual up to the split point, the section displayed No prior state measurements.

Input layout variants

The Input Data section was dynamically structured according to the task type. Most tasks used a single chronological event list under a Discrete Event Sequence header, followed by a Continuous State History block. Two task types required split inputs: CONNECT_POINTS organized the input into Known History (events up to the start point) and Target Future State (the single anchor event), while IMPUTE_RANGE organized the input into History Before Gap and History After Gap. Tasks that did not use state information (ANOMALY_DETECTION, IMPLICIT_REMOVAL, REORDERING, STATE_IMPUTATION) omitted the state-history block entirely.

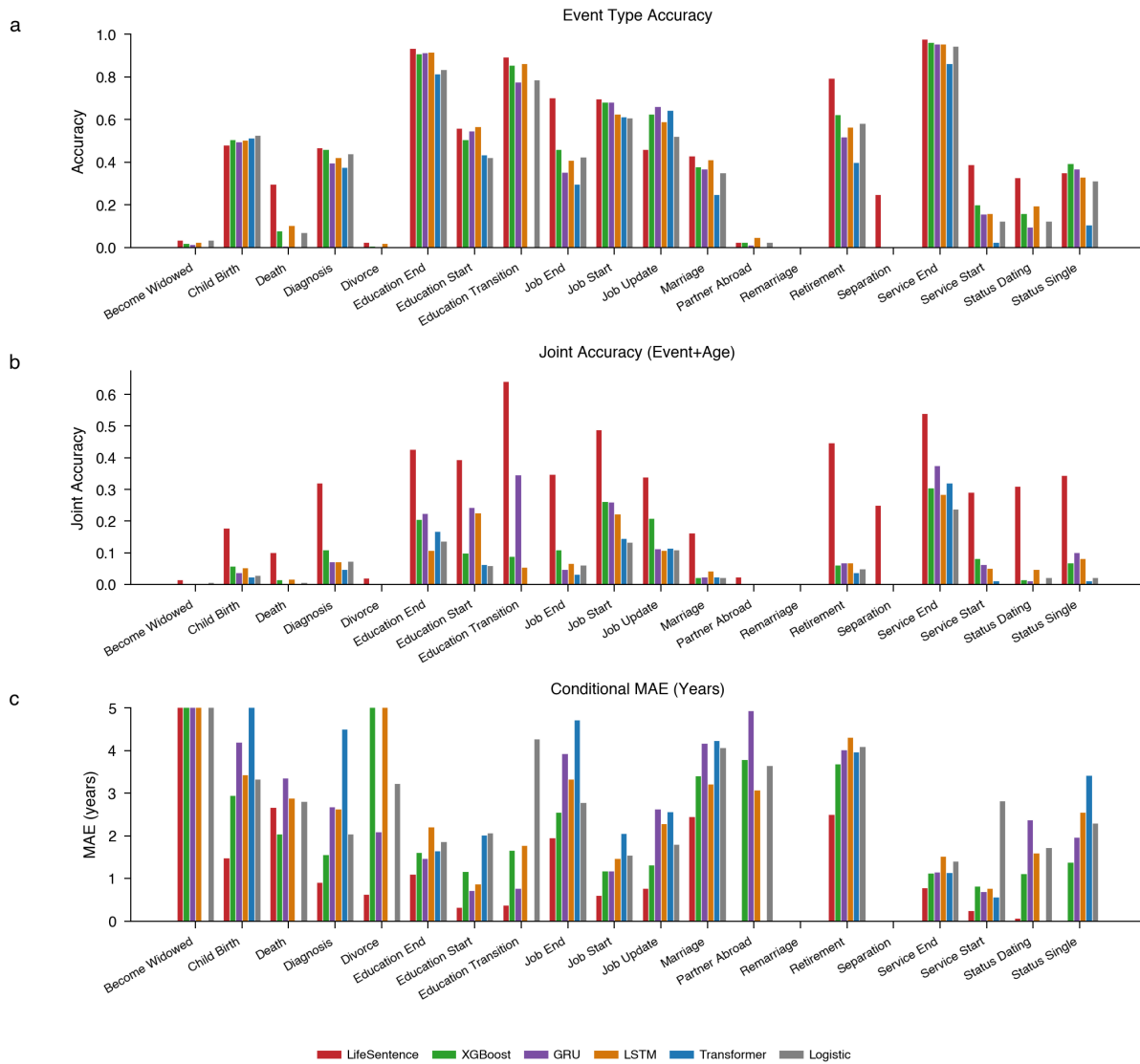
Supplementary Figures



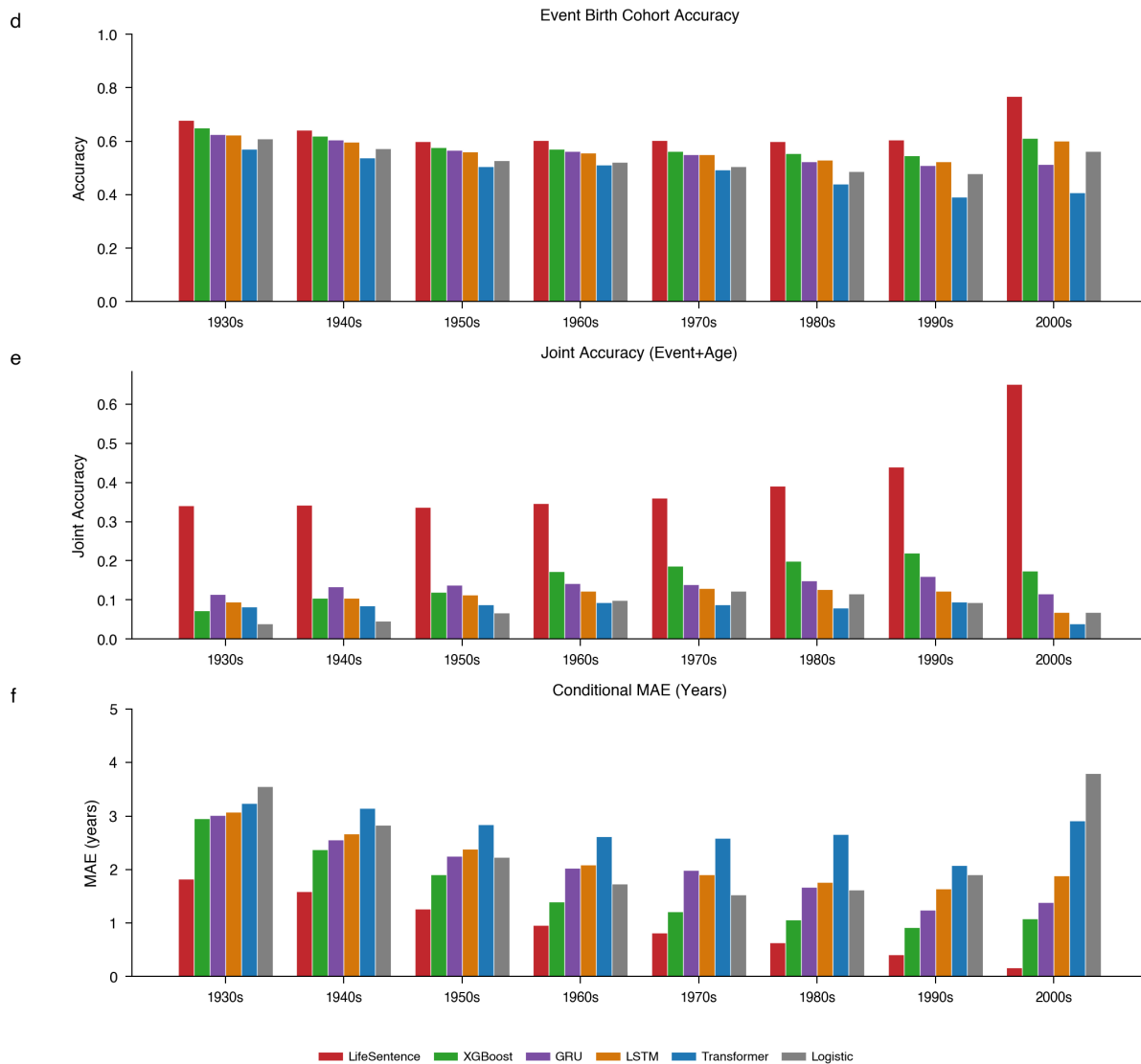
Supplementary Figure 1 — Age-stratified predictive performance on the next-event task. (a) Event type accuracy, (b) joint accuracy (correct event type and age within one year), and (c) conditional mean absolute error (MAE, in years, computed only for correctly predicted event types) as a function of the current age at which the individual's history is truncated. All models exhibit reduced accuracy during the 20–30 age range, consistent with this period's characterization as a demographically dense interval of concurrent life transitions. LifeSentence (blue) maintains substantially higher performance across all age ranges and metrics. The advantage is most pronounced for joint accuracy, where LifeSentence sustains values above approximately 25% even at peak volatility (ages 20–30), while all baselines remain below 15%. Conditional MAE remains near or below one year for LifeSentence across the full age range, whereas baseline models exhibit errors of two to four years.

Model	Jaccard Similarity	Multiset Jaccard	Levenshtein Distance	Wasserstein Distance
LifeSentence	0.627 [0.625-0.629]	0.437 [0.435-0.439]	8.103 [8.032-8.174]	5.211 [5.168-5.252]
Transformer	0.369 [0.367-0.372]	0.092 [0.091-0.093]	27.225 [27.202-27.247]	11.580 [11.511-11.649]
LSTM	0.528 [0.525-0.530]	0.143 [0.142-0.144]	26.189 [26.163-26.216]	19.402 [19.279-19.521]
GRU	0.524 [0.522-0.526]	0.233 [0.232-0.234]	19.456 [19.383-19.528]	14.674 [14.602-14.750]
XGBoost	0.520 [0.518-0.522]	0.275 [0.273-0.277]	19.867 [19.716-20.019]	7.490 [7.438-7.541]
Logistic	0.496 [0.494-0.498]	0.174 [0.172-0.175]	32.315 [32.162-32.479]	12.756 [12.674-12.838]

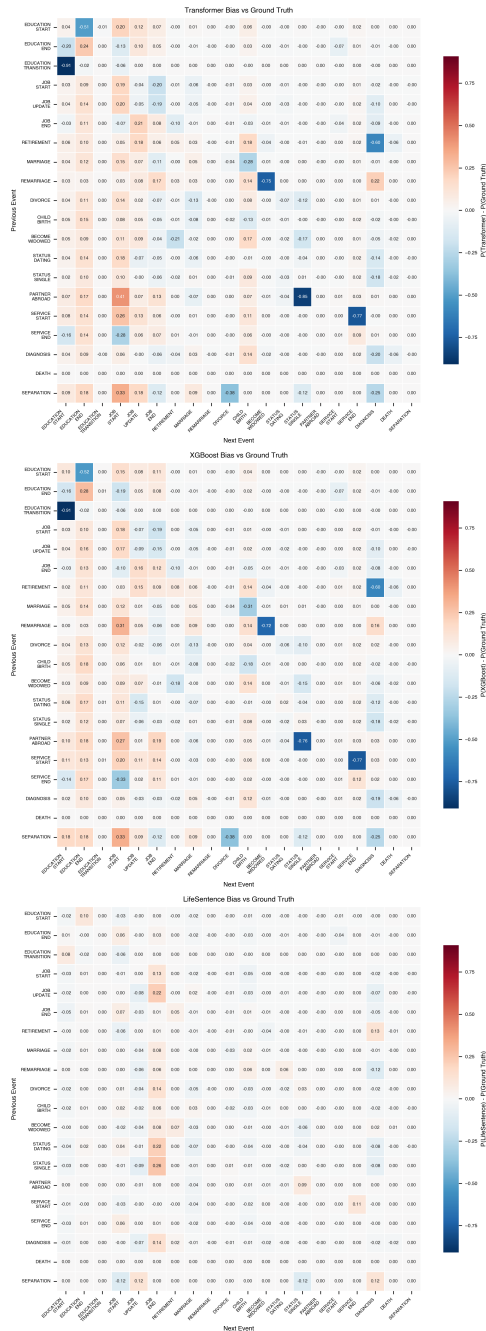
Supplementary Table 2 — Structural fidelity of generated life trajectories. Comparison of LifeSentence against baseline models on the entire trajectory generation task. Metrics include Jaccard Similarity (measuring the overlap of unique event types), Multiset Jaccard (accounting for frequency of repeated events), Levenshtein Distance (minimum edit distance to transform the predicted sequence into the ground truth), and Wasserstein Distance (measuring the cost to move predicted events to their correct temporal positions). 95% confidence intervals (in brackets) were calculated via 1000 bootstrapped samples. LifeSentence outperforms all baselines across all metrics, indicating superior narrative and temporal coherence.



Supplementary Figure 2 — Next-event prediction performance stratified by event type and birth cohort. (a–c) Performance by event type. (a) Event type accuracy, (b) joint accuracy (correct event type and age within one year), and (c) conditional mean absolute error (MAE, in years) across all 15 event categories. LifeSentence (blue) achieves the highest accuracy for the majority of event types, with its advantage most pronounced for socially normative events with well-defined temporal windows. Notably, divorce and death remain difficult for all models, reflecting low base rates and high temporal variance. LifeSentence's conditional MAE is consistently the lowest across event types, with near-zero errors for service start and service end, indicating precise temporal placement for institutionally bounded events. All models struggle with the timing of relationship status changes (dating, single), consistent with the high entropy of these transitions.

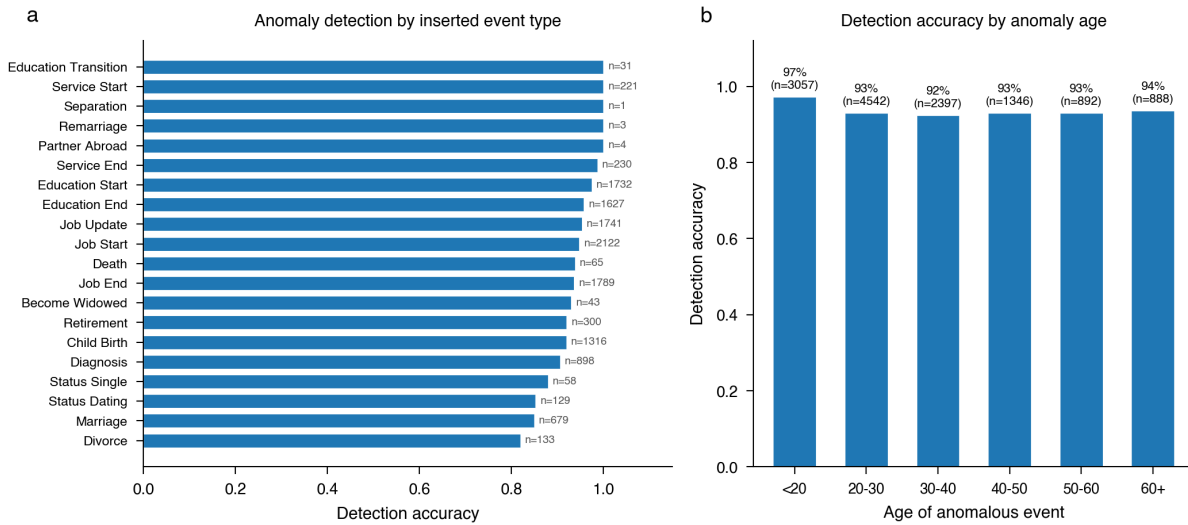


Supplementary Figure 2 (continued) — Next-event prediction performance stratified by birth cohort (d–f) Performance by birth cohort. (d) Event type accuracy, (e) joint accuracy, and (f) conditional MAE for individuals grouped by birth decade (1930s–2000s). LifeSentence maintains a stable advantage across all cohorts, and its joint accuracy and conditional MAE improve for more recent cohorts (1980s–2000s), likely reflecting denser observation windows and more complete event histories for younger individuals within the SOEP panel. Baseline models show comparatively flat or inconsistent trends across cohorts. The consistency of LifeSentence's advantage across both cohorts and event types indicates that the model captures generalizable temporal dependencies rather than overfitting to cohort-specific or event-specific patterns.



Supplementary Figure 3 — Transition matrix residuals for baseline and LifeSentence models.

Each panel displays the difference between a model's predicted transition probabilities and the ground truth transition probabilities ($P(\text{Model}) - P(\text{Ground Truth})$) for all pairwise event sequences. Rows indicate the preceding event, and columns indicate the next event. Red cells denote overprediction (the model assigns higher probability to that transition than observed empirically) and blue cells denote underprediction. All three panels share a common colour scale (-.8 to +.8) to enable direct visual comparison. (a/b) The residual matrices exhibit large errors concentrated in deterministic transition pairs. The models massively underpredict the SERVICE_START → SERVICE_END transition and the RETIREMENT → DIAGNOSIS transition, indicating a failure to learn that institutionally and biographically paired events follow each other with high probability. (c) LifeSentence. The residual matrix is markedly sparser and closer to zero. The largest remaining errors involve moderate overprediction of JOB_END following relationship status events such as STATUS_DATING (+0.22) and STATUS_SINGLE (+0.26). Critically, LifeSentence resolves the deterministic transition failures that dominate the baseline models: the SERVICE_START → SERVICE_END error is reduced to +0.11, confirming that the model has learned the closure constraints of institutionally bounded event pairs.



Supplementary Figure 4 — Anomaly detection performance by event type and age. (a) Detection accuracy stratified by the type of anomalous event inserted into the trajectory. Events embedded in institutional sequences (e.g., SERVICE_START, EDUCATION_TRANSITION, REMARRIAGE) are detected at near-perfect rates, whereas relationship transitions (e.g., DIVORCE, MARRIAGE) prove more difficult to identify, reflecting greater inter-individual variability in their timing and occurrence. (b) Detection accuracy stratified by the age at which the anomalous event was inserted. Accuracy is highest for events inserted before age 20 (97%), dips modestly during the 20–30 window of high demographic activity (92%), and stabilises at approximately 93% across subsequent life stages. Sample sizes are shown in parentheses. Overall accuracy: 93.93%.

Task	Model	Event Accuracy	Joint Accuracy	Age MAE
Next 3 Events	LifeSentence	0.462 [0.459-0.465]	0.200 [0.198-0.202]	1.74 [1.71-1.77]
Next 3 Events	XGBoost	0.437 [0.434-0.440]	0.083 [0.081-0.084]	2.57 [2.54-2.60]
Next 3 Events	GRU	0.425 [0.422-0.428]	0.078 [0.077-0.080]	3.24 [3.21-3.28]
Next 3 Events	LSTM	0.419 [0.416-0.422]	0.059 [0.058-0.061]	3.29 [3.26-3.32]
Next 3 Events	Transformer	0.384 [0.381-0.387]	0.054 [0.052-0.055]	3.34 [3.31-3.37]
Next 3 Events	Logistic	0.397 [0.394-0.399]	0.052 [0.050-0.053]	3.20 [3.16-3.23]
Next Specific Type	LifeSentence	—	0.213 [0.209-0.218]	4.23 [4.18-4.29]

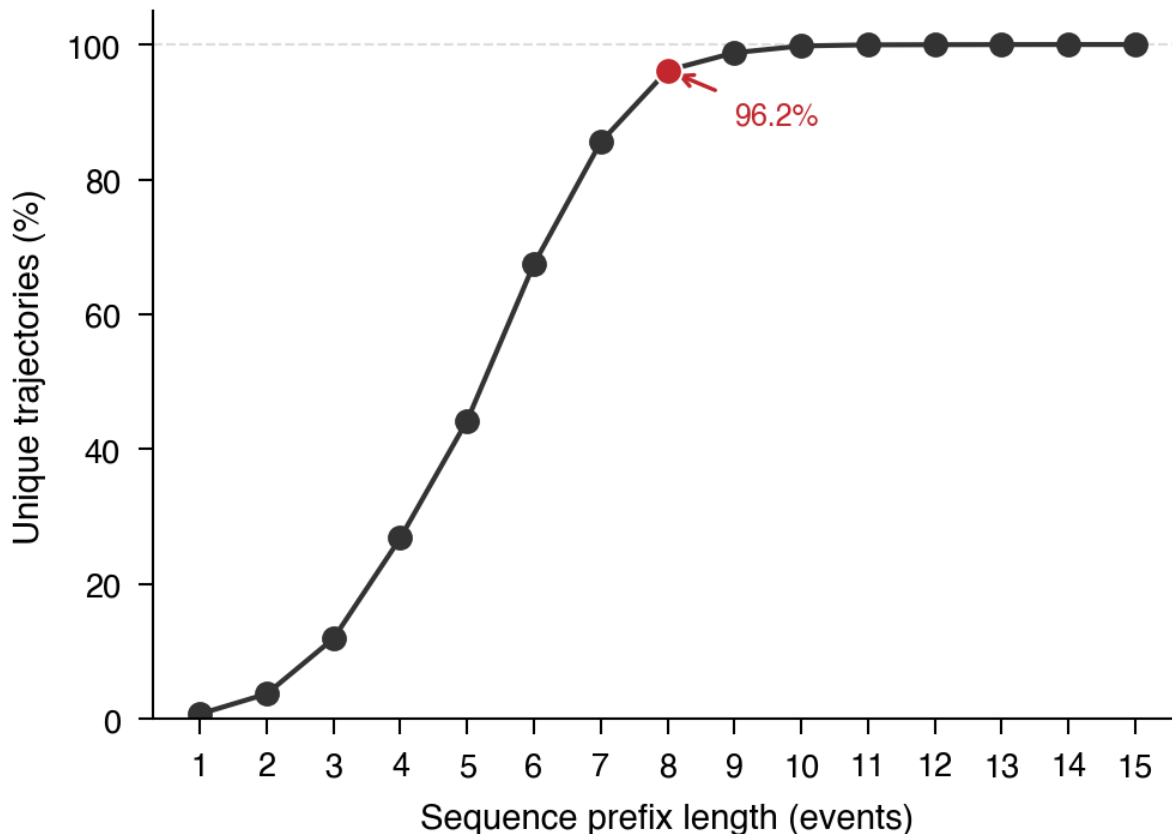
Supplementary Table 3a — Short-horizon and event-targeted constrained prediction.

Next-3-Events task: accuracy of predicting the next three life events in sequence following a random truncation point in the individual's history. Event Accuracy measures whether each of the three predicted event types matches the ground truth event at the same position. Joint Accuracy measures the probability that a predicted event is both the correct type and occurs at the correct age (within rounding to nearest year). Age MAE reports the mean absolute age error conditional on correct event type prediction. Next Specific Type task (LifeSentence only): the model is given the target event type and asked to predict only when it will occur; event accuracy is therefore 100% by construction and not reported. Joint Accuracy for this task is the proportion of predictions within one year of the ground truth age. LifeSentence outperforms all baselines on all Next-3-Events metrics. The Next Specific Type task is evaluable only for LifeSentence as it requires natural-language instruction following to specify the target event type. 95% confidence intervals (in brackets) were calculated via 1,000 bootstrap samples across all three prediction positions.

Task	Model	Constraint Satisfaction	Jaccard	Levenshtein	Wasserstein
Predict Until Event	LifeSentence	0.993 [0.992–0.994]	0.650 [0.646–0.653]	4.19 [4.11–4.26]	4.67 [4.60–4.73]
Predict Until Event	LSTM	0.792 [0.786–0.797]	0.543 [0.540–0.547]	9.31 [9.19–9.43]	7.59 [7.50–7.67]
Predict Until Event	XGBoost	0.754 [0.748–0.760]	0.542 [0.538–0.545]	8.78 [8.66–8.90]	6.18 [6.12–6.25]
Predict Until Event	GRU	0.713 [0.706–0.719]	0.527 [0.524–0.531]	11.88 [11.73–12.04]	7.43 [7.34–7.52]
Predict Until Event	Logistic	0.600 [0.594–0.607]	0.495 [0.492–0.498]	13.40 [13.25–13.55]	9.14 [9.04–9.25]
Predict Until Event	Transformer	0.446 [0.440–0.452]	0.398 [0.394–0.401]	17.37 [17.20–17.53]	7.94 [7.86–8.02]
Predict Up To Year	LifeSentence	0.917 [0.915–0.920]	0.559 [0.556–0.562]	2.25 [2.24–2.27]	1.84 [1.81–1.87]
Predict Up To Year	XGBoost	0.443 [0.438–0.448]	0.441 [0.438–0.444]	5.24 [5.17–5.30]	2.14 [2.11–2.16]
Predict Up To Year	GRU	0.024 [0.022–0.025]	0.402 [0.399–0.404]	4.71 [4.66–4.76]	2.66 [2.63–2.69]
Predict Up To Year	Logistic	0.358 [0.353–0.363]	0.382 [0.379–0.384]	5.66 [5.60–5.73]	2.39 [2.36–2.41]
Predict Up To Year	Transformer	0.096 [0.093–0.099]	0.311 [0.308–0.314]	7.48 [7.41–7.55]	3.12 [3.07–3.16]
Predict Up To Year	LSTM	0.038 [0.036–0.040]	0.377 [0.374–0.379]	4.25 [4.21–4.29]	2.60 [2.57–2.63]
Snapshot Year	LifeSentence	99.9% [99.9–100.0%]	0.429 [0.425–0.434]	0.84 [0.84–0.85]	
Connect Points	LifeSentence	94.6% [93.9–95.3%]	0.587 [0.580–0.595]	7.08 [6.85–7.32]	7.91 [7.75–8.07]

Supplementary Table 3b — Sequence generation under temporal and semantic constraints.

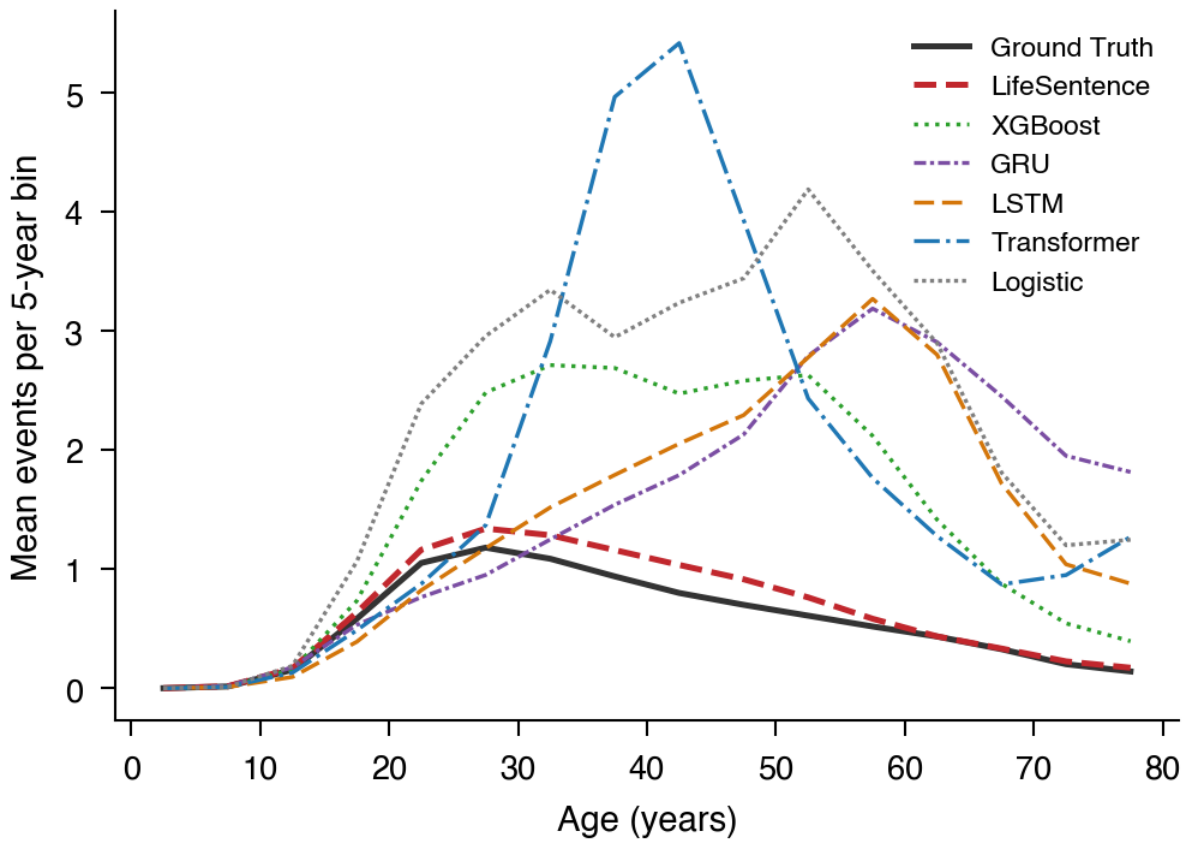
Predict Until Event: the model generates all future life events up to and including a specified milestone event (death, retirement, or marriage). Constraint Satisfaction reports whether the trajectory generates up to the appropriate event/year. Predict Up To Year: the model generates all events occurring before a specified calendar year. Jaccard measures overlap of unique predicted event types against ground truth; Levenshtein Distance measures the minimum sequence edit distance on event-type strings; Wasserstein Distance measures the temporal displacement cost of optimally matching predicted event ages to ground-truth positions. LifeSentence achieves the highest Jaccard and lowest Levenshtein and Wasserstein distances across all tasks where comparison is possible. Baseline models satisfy the Predict Until Event milestone constraint at rates between 44.6% (Transformer) and 79.2% (LSTM) — substantially above zero, but achieved through overgeneration rather than targeted termination, as reflected in their substantially worse Jaccard and Levenshtein scores. Snapshot Year and Connect Points are evaluable only for LifeSentence, as both tasks require semantic instruction following: Snapshot Year asks the model to generate only events occurring during a specified future calendar year, while Connect Points provides an early life history and a single distant anchor event and asks the model to generate the intervening multi-decade trajectory. 95% confidence intervals (in brackets) were calculated via 1,000 bootstrap samples.



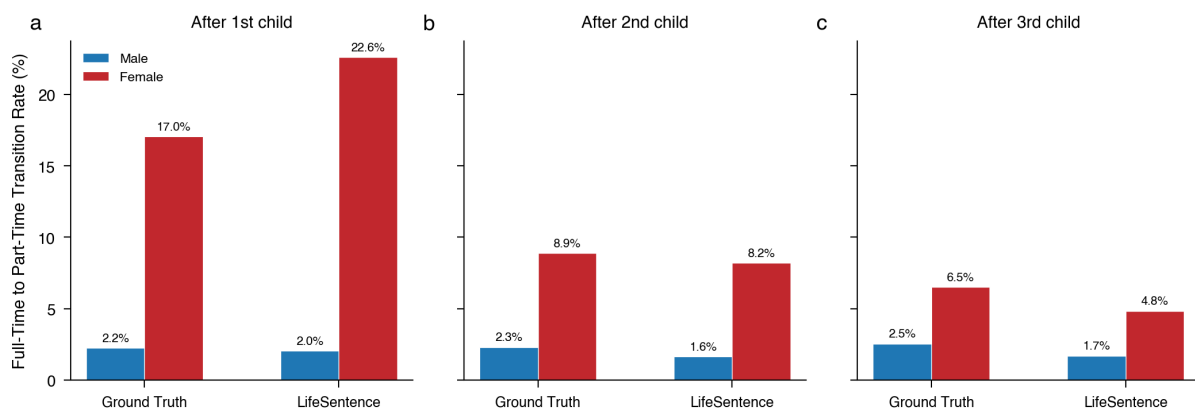
Supplementary Figure 5 — Combinatorial complexity of human life trajectories. Percentage of unique event-type sequences in the dataset as a function of sequence prefix length (number of events). Uniqueness rises steeply: by the 8th event, 96.2% of individuals possess a life trajectory shared by no other person in the dataset, and by the 10th event the figure approaches 99.8%. This combinatorial growth means that the model cannot rely on memorised templates when generating complete trajectories. Each predicted biography must be constructed from learned principles of temporal and causal structure rather than retrieved from training examples, underscoring the difficulty of the trajectory generation task.

Model	Masked History	Implicit Gap	Masked Period
LifeSentence	0.539 [0.534-0.544]	0.496 [0.491-0.501]	0.455 [0.448-0.461]
XGBoost	0.437 [0.432-0.443]	0.433 [0.428-0.438]	0.363 [0.357-0.369]
GRU	0.424 [0.419-0.429]	0.421 [0.416-0.427]	0.352 [0.346-0.358]
LSTM	0.416 [0.411-0.421]	0.413 [0.407-0.418]	0.338 [0.332-0.344]
Transformer	0.382 [0.377-0.387]	0.376 [0.371-0.381]	0.324 [0.317-0.329]
Logistic	0.396 [0.390-0.401]	0.390 [0.385-0.395]	0.324 [0.318-0.330]

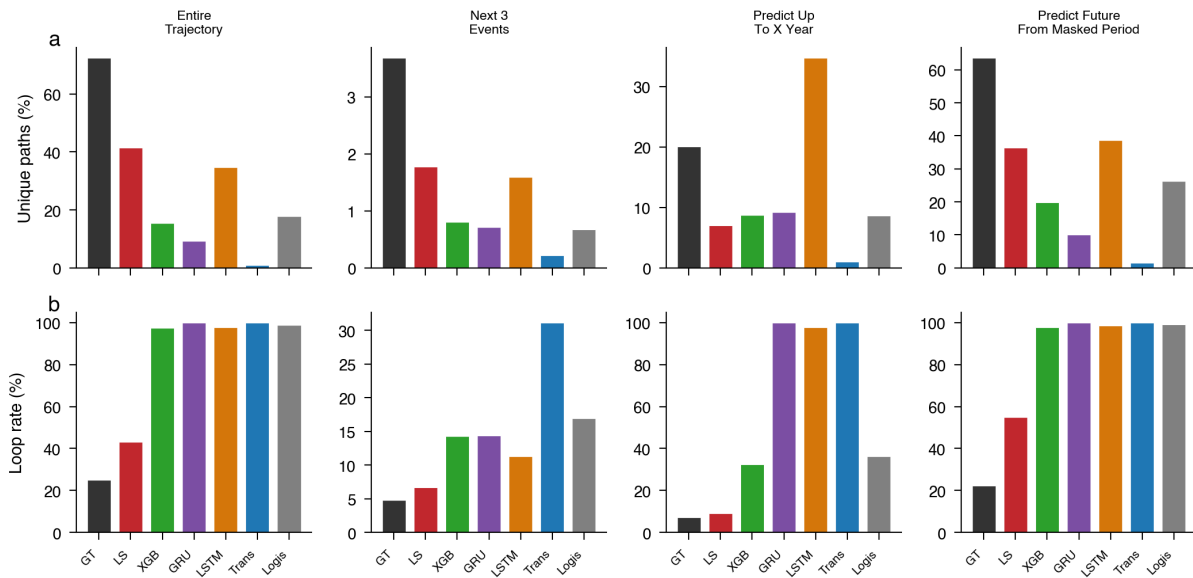
Supplementary Table 4 — Robustness of next-event prediction under missing historical information. Next-event type accuracy for LifeSentence and baseline models across three masking tasks of increasing severity. Masked History: random individual events in the history are replaced with a [MASKED EVENT] token, preserving sequence length but removing content. Implicit Gap: events are silently deleted without markers, simulating realistic data collection gaps where missingness is unobservable. Masked Period: a continuous temporal window of events is removed, simulating extended observational blackouts. LifeSentence maintains the highest accuracy across all three conditions. Notably, the Transformer baseline performs worst across all conditions, falling below even the Logistic regression on Masked History (0.382 vs 0.396), suggesting that the from-scratch Transformer's learned representations are more fragile to missing inputs than simpler models. 95% confidence intervals (in brackets) were calculated via 1000 bootstrapped samples.



Supplementary Figure 6 — Temporal density of life events. Comparison of the mean number of predicted events per year across age bins for LifeSentence, Ground Truth, and baseline models. LifeSentence accurately reproduces the non-linear peak in demographic activity between ages 25 and 30, matching the ground truth distribution.

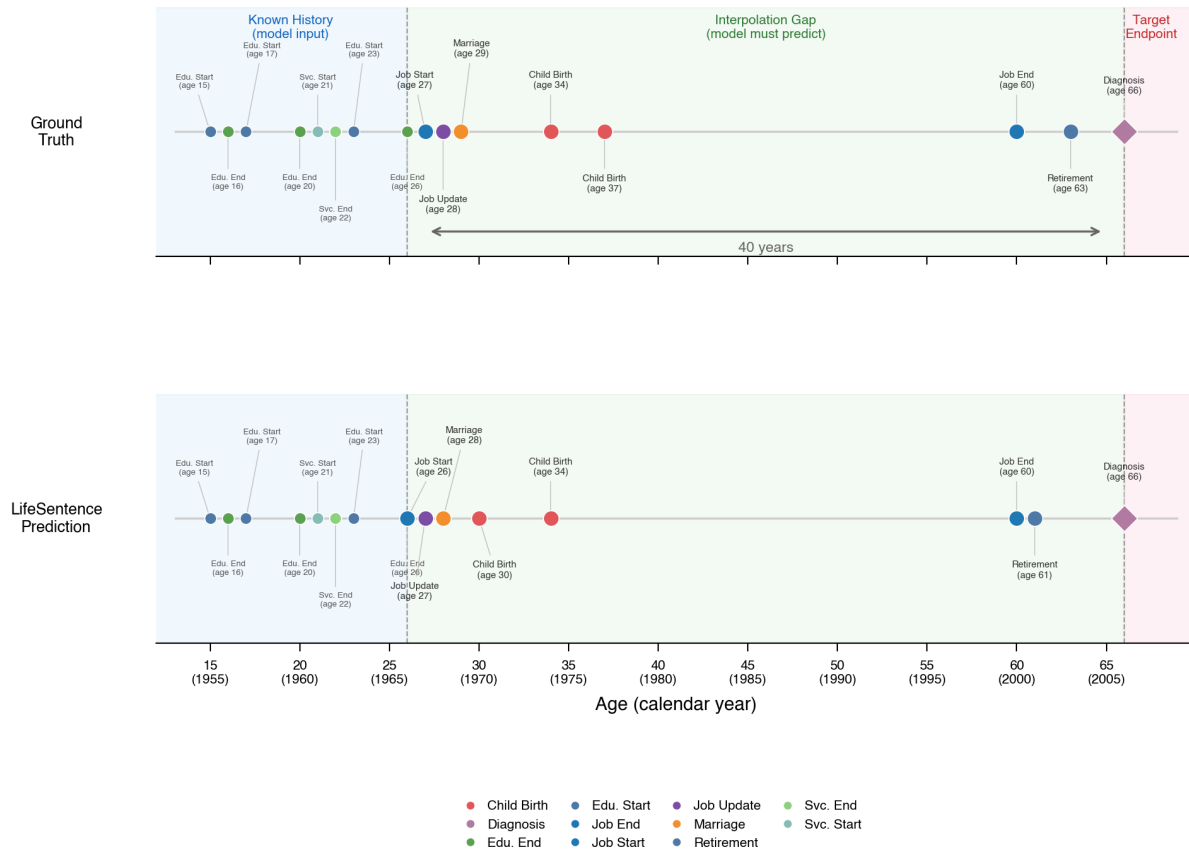


Supplementary Figure 7 | Part-Time Work Transition After Childbirth Across Gender. The proportion of individuals who transition from full-time to part-time employment specifically following the birth of child, stratified by sex. The model correctly predicts a significantly higher transition rate for females compared to males.

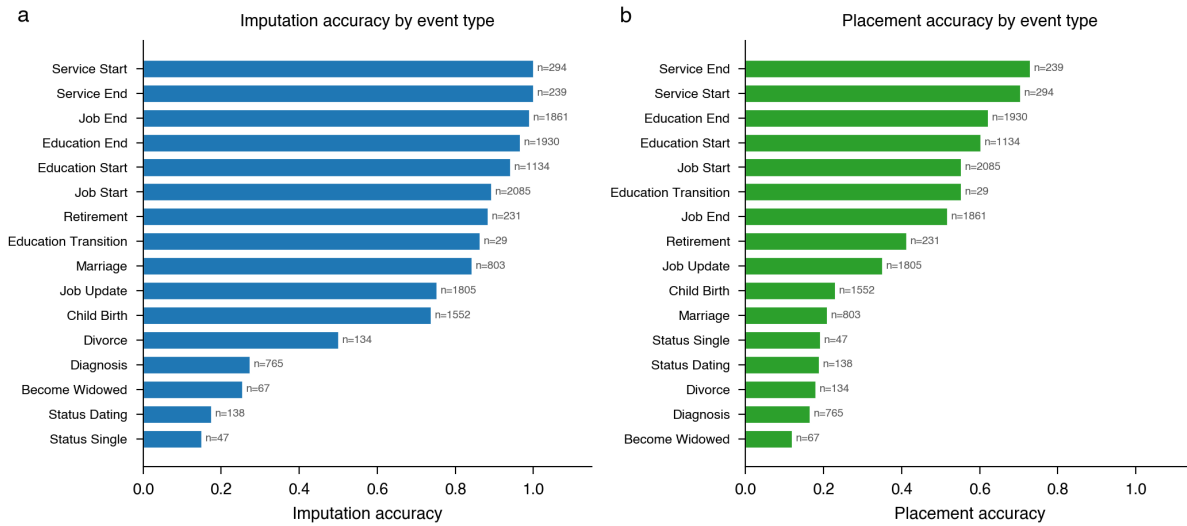


Supplementary Figure 8 — Comparative analysis of generative diversity and structural integrity. (a) Comparison of unique life path diversity, showing that LifeSentence generates a wider array of distinct biographical sequences compared to the Transformer baseline, which suffers from mode collapse. (b) Frequency of repetitive loop artifacts (e.g., illogical repetitions of the same life event or patterns). LifeSentence demonstrates a marked reduction in looping behavior.

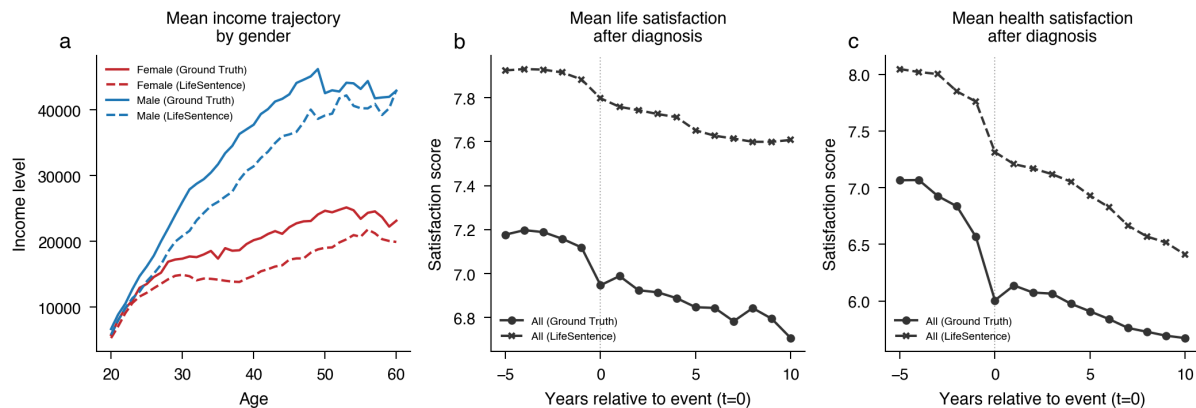
Trajectory interpolation example



Supplementary Figure 9 — Trajectory interpolation across a 40-year observational gap. Prediction for a single individual (male, born 1940), in which the model receives the observed history up to age 25 (left of dashed line) and a single target endpoint (Diagnosis at age 66, red diamond) and must generate the intervening sequence of life events spanning four decades. Top row: ground truth trajectory. Bottom row: LifeSentence prediction. The model recovers every event type in the correct order (Levenshtein distance = 0, Jaccard = 1.00), reconstructing the canonical male life-course arc — job entry and career updating in the late 20s, marriage followed by two childbirths through the 30s, a long period of occupational stability, and job end preceding retirement in the early 60s — with a mean temporal displacement of only 1.71 years (Wasserstein distance). The largest timing errors occur in the family formation window, where the model places marriage and first childbirth approximately four years earlier than observed (predicted ages 28 and 30 versus ground truth ages 29 and 34). This example illustrates that when provided with early biographical context and a late-life anchor, LifeSentence can reconstruct the intermediate trajectory with high fidelity, leveraging the structural constraints of the life course — that education precedes employment, which precedes family formation, which precedes retirement — to fill a 40-year gap.



Supplementary Figure 10 — Imputation accuracy for silently deleted events, stratified by event type. (a) Imputation accuracy: assessing whether LifeSentence correctly identifies the event type from the surrounding trajectory context alone. Events embedded in deterministic institutional sequences — service end (1.00), service start (1.00), job end (0.99), education end (0.96) — are recovered at near-perfect rates, as their absence creates an unmistakable logical gap (e.g., a service start without a corresponding service end). Accuracy declines through events with greater inter-individual variability in timing and occurrence, such as childbirth (0.74) and divorce (0.50), and is lowest for high-entropy relational states — diagnosis (0.27), widowhood (0.25), dating status (0.17), and single status (0.15) — whose presence or absence is weakly constrained by the surrounding event sequence. (b) Placement accuracy: the proportion of correctly identified events that are also placed at the correct temporal position within the trajectory. The rank ordering largely mirrors imputation accuracy — institutionally anchored events such as service end (0.73) and service start (0.70) are easiest to place, while life events with variable timing such as marriage (0.21), diagnosis (0.16), and widowhood (0.12) are hardest — but placement accuracy is uniformly lower, reflecting the additional difficulty of inferring when a missing event occurred rather than simply what it was. Together, these panels reveal that events governed by institutional structure are both identifiable and temporally localizable from context, while events with higher inter-individual variability leave weaker contextual traces.



Supplementary Figure 11 — Emergent sociodemographic stratification and event-driven perturbations in continuous state predictions. (a) Mean predicted income trajectories across the lifespan stratified by gender, comparing ground truth (solid lines) with LifeSentence predictions (dashed lines) for male (blue) and female (red) individuals. The model recovers the gender income gap without explicit supervision: male trajectories exhibit steeper growth through early and mid-career, while female trajectories follow a flatter curve at lower levels. LifeSentence preserves the relative magnitude and temporal shape of the divergence across the working life. (b–c) Mean satisfaction scores in the years surrounding a diagnosis event ($t = 0$, dotted vertical line), comparing ground truth (solid lines with circle markers) with LifeSentence predictions (dashed lines with cross markers). (b) Life satisfaction shows a modest decline following diagnosis, which the model captures directionally while slightly overestimating absolute levels. (c) Health satisfaction exhibits a sharper and more sustained decline after diagnosis, with LifeSentence reproducing the overall downward slope and post-diagnosis trajectory. In both cases, the model systematically overestimates absolute satisfaction but accurately recovers the direction, timing, and relative magnitude of diagnosis-induced perturbations, indicating that the relationship between discrete health events and subjective well-being is sufficiently structured within biographical sequences to be learned from observational data alone.